# KAPITEL 1 / *CHAPTER 1* [1]
# MATHEMATICAL MODELING OF FREQUENCY TRANSDUCERS OF THE RADIO MEASURING DEVICE OF MAGNETIC FIELD INDUCTION

**DOI: 10.30890/2709-2313.2023-18-03-014**

## Introduction

Measuring magnetic field induction as a characteristic of the magnetic field is one of the most important tasks in the field of creating and ensuring the functioning of navigation, orientation and stabilization systems; shielding of quantum computers, magnetic tomography, flaw detection and non-destructive testing of products, as well as implementation of security and protection systems of various objects. High-precision magnetic field measuring devices are also used for searching and detecting magnetic anomalies in space, in the air, underwater, surface and underground environments, during geophysical and geological monitoring, measuring large currents, etc. [1 – 7]. Magnetic fields are usually divided into super-strong (over 100 T), strong (from 4 to 100 T), medium (from 0.05 to 4 T), and weak (less than 0.05 T) [1, 2]. Depending on the field of application of the magnetometer and the value of the measured magnetic field, the problem of choosing one or another primary measuring transducer of the magnetic field arises. The development of modern mobile robotic complexes for both terrestrial, underwater and space purposes requires anticipatory development of magnetometers with high sensitivity for measuring weak magnetic fields and use as part of navigation, orientation and stabilization systems [8-10]. Very often, the measurement of the induction of the magnetic field must be carried out under the influence of external disturbances of the Earth's magnetic field.

Currently, many devices have been developed for measuring magnetic field parameters. Among them there are also very sensitive - SQUIDS. But they have not received practical application, for example, in navigation systems, in military intelligence to determine the location of sunken submarines, in geology, since these devices require cryogenic equipment, which limits the scope of their use. Thus, there is a need to develop devices that will meet the requirements of energy consumption, sensitivity, geometric dimensions and mass, which will allow solving the above problems more accurately and qualitatively.

The magnetic field sensor is a sensitive element of any magnetometer and is designed to convert the measured value of the magnetic field into an electrical signal, most often into a voltage [7, 8].

[1]***Authors:*** *Osadchuk Oleksandr Volodymyrovych, Osadchuk Volodymyr Stepanovych, Prytula Maksym Oleksandrovych, Osadchuk Iaroslav Oleksandrovych*

One of the main components of measuring devices is a sensor, which can consist of two key elements: a sensitive element and a special scheme for processing the output signal of the sensitive element (transducer, buffer stage), which depends on the specifics of the device's application. The signal processing scheme is necessary to convert the analog signal of the sensitive element into a form suitable for coordination with control and measurement units. Most often, the main elements of processing circuits are amplifiers and analog-to-digital transducers, but there are other approaches. In particular, the use of frequency conversion in the magnetic field sensor allows to increase the sensitivity of the sensor [8, 11-16].

Based on the above, a promising scientific direction is the development and creation of magnetic field induction measuring devices that use semiconductor sensors with self-generating frequency transducers [14, 15-18]. The use of an autogenerator frequency transducer with a semiconductor magnetosensitive element as a sensor of a radio measuring device allows you to compensate for active losses in the device and increase the transmission coefficient of the measuring transducer. Thus, the improvement of highly sensitive magnetic field induction measuring devices, which include a frequency transducer with a magnetosensitive element, is an actual direction of scientific research [17].

## 1.1. Mathematical model of the radio-measuring frequency transducer of the magnetic field based on the Hall element and transistor structure on field-effect and bipolar transistors

Since the main element that determines the sensitivity of the measuring device in this case is a frequency transducer with a semiconductor magnetosensitive element, we will focus on improving their mathematical models with three different circuit solutions.

To determine the theoretical characteristics and conversion functions of radio measuring transducers, it is necessary to create a mathematical model of the proposed schematic solutions of the transducers. The first schematic solution is shown in fig. 1.

In this schematic solution, a Hall sensor is used as a magnetically sensitive element, an active inductance is built on transistor VT3, and a controlled equivalent capacitance is built on transistors VT1 and VT2. The principle of operation of this radio-measuring frequency transducer of the magnetic field with a frequency output is based on the change in the generation frequency of the transducer depending on the change in the level of the informative signal (which depends on the induction of the

measured magnetic field) from the Hall sensor. For this purpose, the equivalent scheme of fig. 2 with MOSFET and bipolar transistors, and with a Hall sensor as a sensitive element [21].

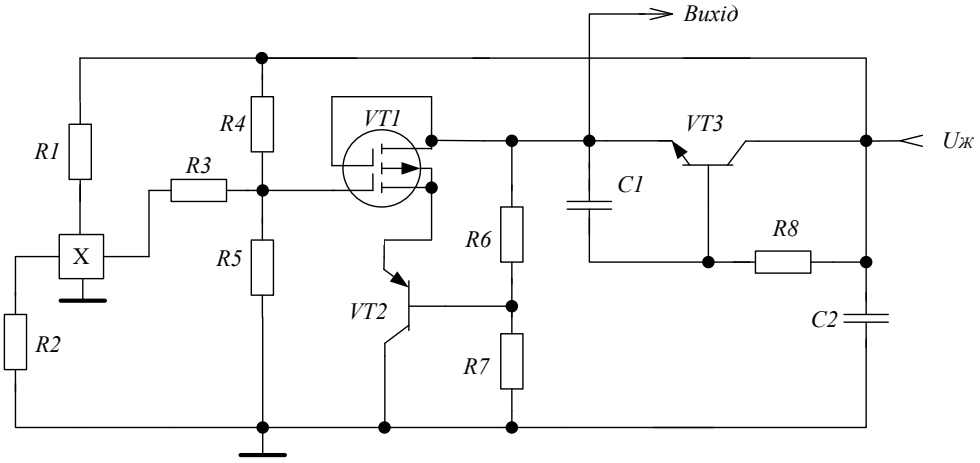


**Figure 1 – Electrical diagram of a radio measuring frequency magnetic field transducer with a Hall sensor**

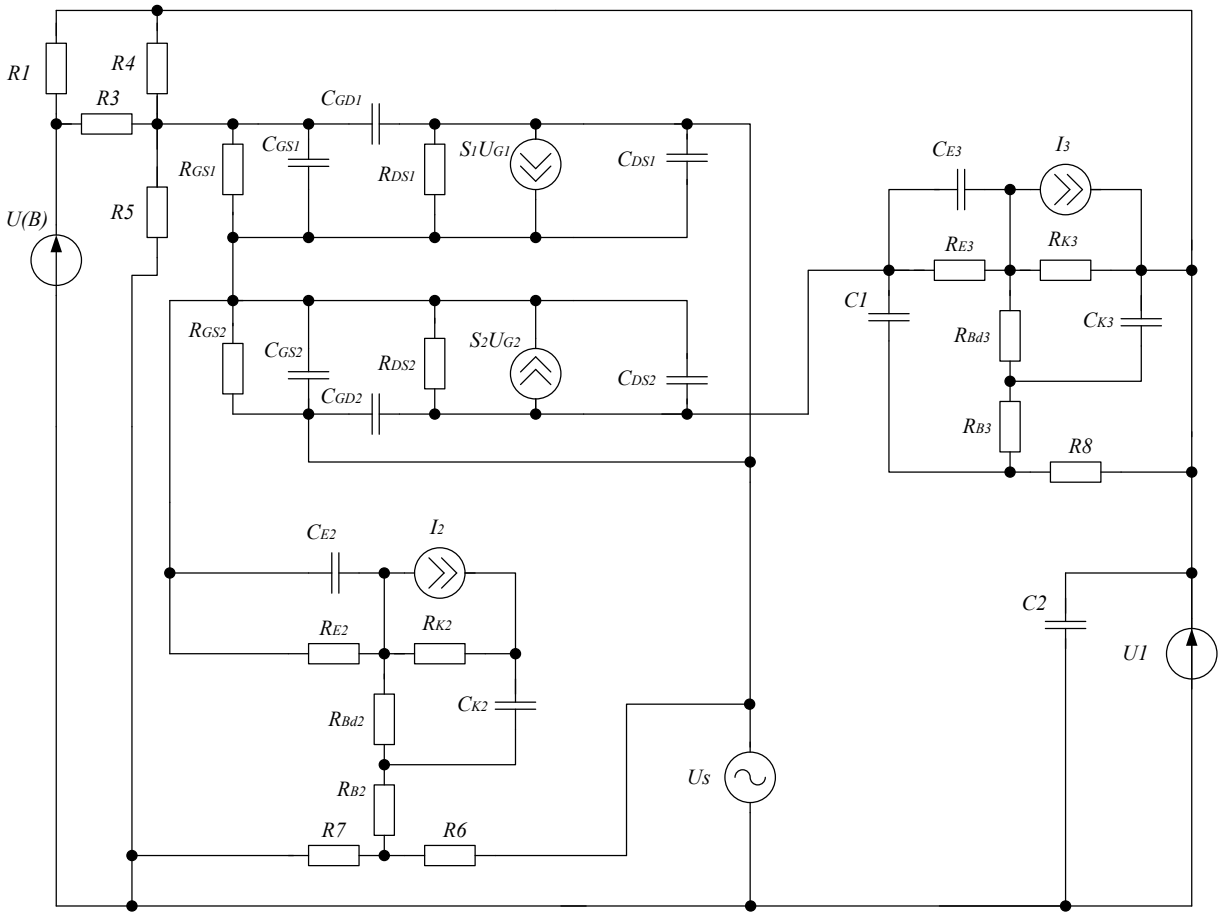


**Figure 2 – Non-linear equivalent circuit of the radio measuring device magnetic field frequency transducer with a Hall sensor**

The main characteristics of the magnetic induction frequency transducer in the

dynamic mode are the dependence of the active and reactive components of the total resistance at the outputs of the drain-collector transistors structure, the conversion function and sensitivity to the action of the magnetic field. The equivalent circuit (Fig. 2) of the magnetic induction radio measuring transducer (Fig. 1) takes into account the nonlinear properties of the circuit, since the oscillator can operate both in linear and non-linear modes.

The equivalent scheme of fig. 2 contains the following elements: $R_G$ – ohmic resistance of the gate electrode; $R_{GS}$ – resistance between the gate and source electrodes; $R_{DS}$ – drain- source resistance; $R_D$ – resistance p-n of the drain transition; $R_S$ – resistance p-n of the source junction; $R_n$ – substrate resistance; $R_B$ – base resistance; $R_C$ – collector transition resistance; $R_E$ – emitter junction resistance; $R_1$, $R_3$, $R_4$, $R_7$, $R_6$ – supports of the divider.

To simplify the scheme of fig. 2, we will convert the elements or their groups into equivalent complex supports, and also use equivalent schemes of substitution of parallel and series connection of elements. Thus, we get the transformed equivalent circuit of fig. 3.

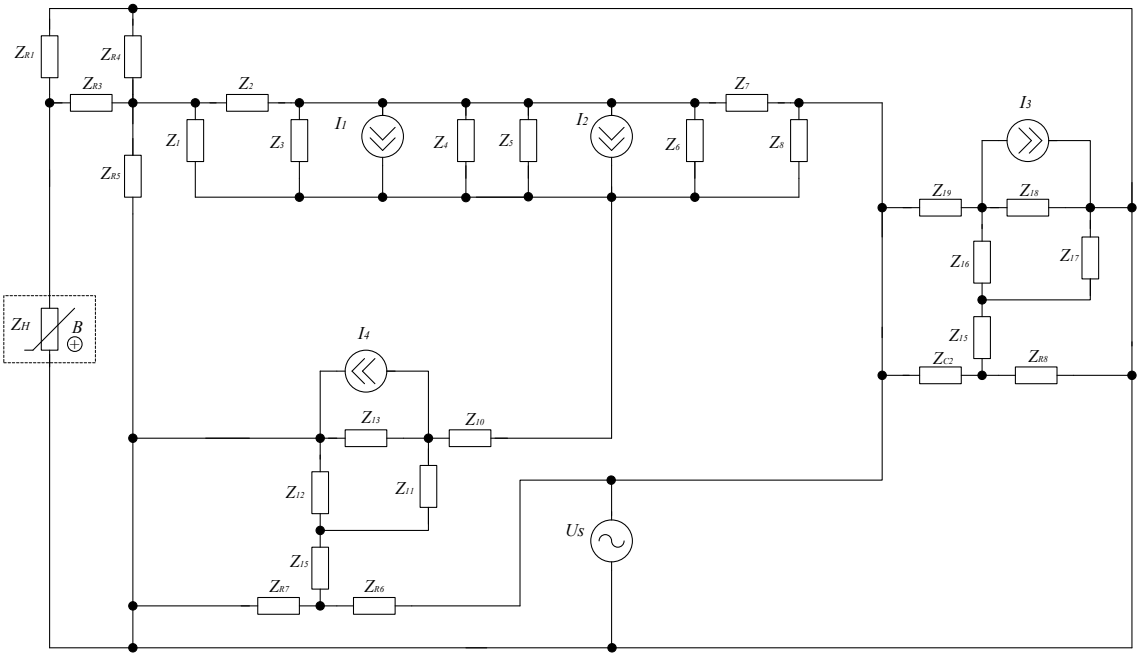


**Figure 3 – Transformed nonlinear equivalent circuit of the magnetic induction frequency transducer**

Having used the complex form of writing for all elements that determine the mode of the circle under alternating current, we will present geometric operations on vectors with their algebraic images, and apply all relations and laws of circles under direct current to the calculation of circles under alternating current. With a complex form of recording, the methods of calculating circles by direct current, such as the method of

loop currents, the method of nodal potentials, the method of transformation, and others, can also be used to calculate circles by alternating current. In the scheme of fig. 3, the following transformations of the complex resistances of the elements are used:

$$Z_1 = \frac{R_{GS_1}}{1+w^2R_{GS_1}^2C_{GS_1}^2} - j\frac{R_{GS_1}^2wC_{GS_1}}{1+wR_{GS_1}^2C_{GS_1}^2}; Z_2 = -\frac{j}{wC_{GD_1}}; Z_3 = R_{DS_1}; Z_{R7} = R_7; Z_4 = -\frac{j}{wC_{DS_1}};$$

$$Z_5 = -\frac{j}{wC_{DS_2}}; Z_6 = R_{DS_2}; Z_7 = -\frac{j}{wC_{GD_2}}; Z_{R4} = R_4; Z_{R6} = R_6; Z_{12} = -\frac{j}{wC_{k_1}}; Z_{13} = R_{k_1}; Z_{14} = R_{B_1};$$

$$Z_8 = \frac{R_{GS2}}{1+w^2R_{GS2}^2C_{GS2}^2} - j\frac{R_{GS2}^2wC_{GS2}}{1+wR_{GS2}^2C_{GS2}^2}; Z_{10} = \frac{R_{E1}}{1+w^2R_{E1}^2C_{E1}^2} - j\frac{R_{E1}^2wC_{E1}}{1+wR_{E1}^2C_{E1}^2}; Z_{11} = R_{Bd_1}; Z_{15} = R_{B_2};$$

$$Z_{16} = R_{Bd_2}; Z_{17} = -\frac{j}{wC_{k_2}}; Z_{18} = R_{k_2}; Z_{R8} = R_8; Z_{19} = \frac{R_{E2}}{1+w^2R_{E2}^2C_{E2}^2} - j\frac{R_{E2}^2wC_{E2}}{1+wR_{E2}^2C_{E2}^2}; Z_{R1} = R_1;$$

$$Z_{R3} = R_3; Z_H = \frac{R_H}{1+w^2R_H^2C_H^2} - j\frac{R_H^2wC_H}{1+w^2R_H^2C_H^2}; Z_{C2} = -\frac{j}{wC_2}.$$

The conversion function of the circuit is the dependence of the frequency of the generated oscillation on the induction of the magnetic field for this circuit solution. To find the transformation function, it is necessary to solve a system of equilibrium equations, the equations of which are composed according to Kirchhoff's laws. We mark the loop currents on the equivalent circuit of fig. 3. The equivalent circuit showing the loop currents is shown in Fig. 4.

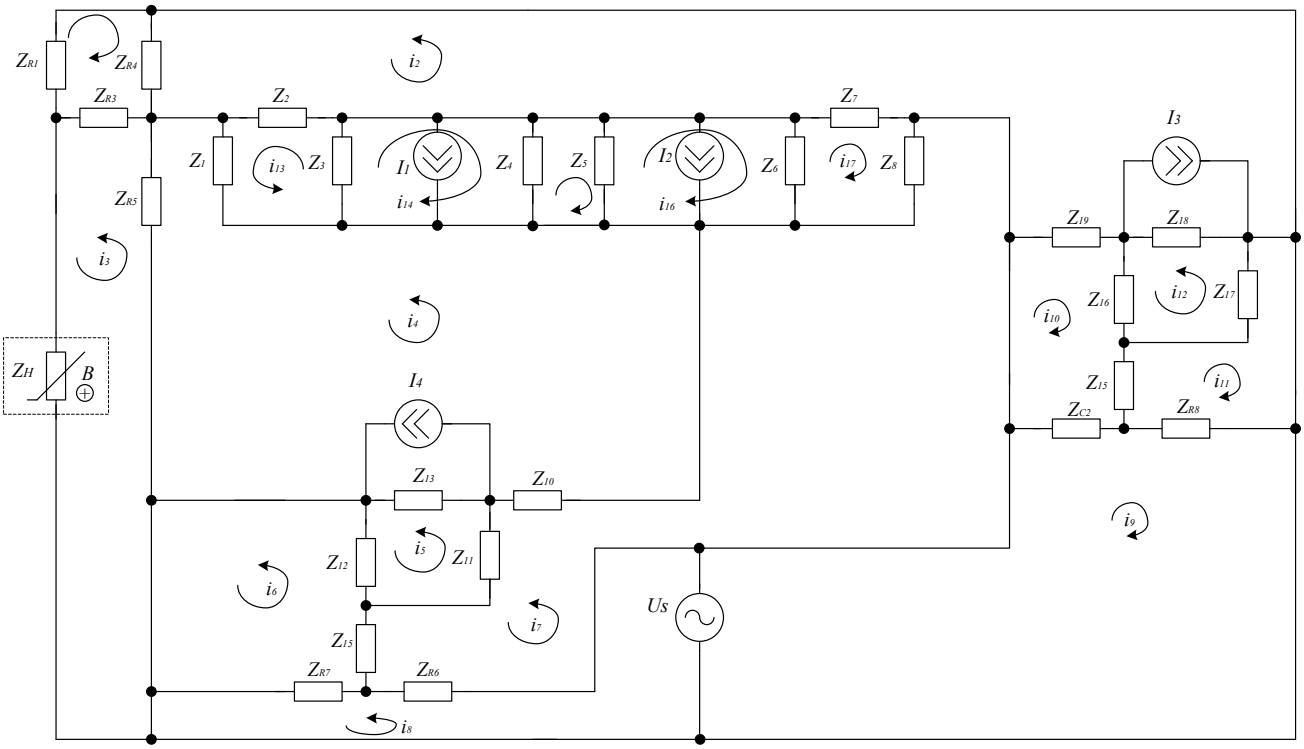


**Figure 4 – Equivalent circuit of the transducer with loop currents**

The system of Kirchhoff equations for the scheme of Fig. 4, according to the directions of the loop currents, has the form:

$$\begin{cases}
0=\left(Z_{11}+Z_{12}+Z_{13}\right)i_5-Z_{11}i_7-Z_{13}\left(I_4+i_4\right)-Z_{12}i_6;\\
0=\left(Z_{R_1}+Z_{R_4}+Z_{R_3}\right)i_1+Z_{R_4}i_2+Z_{R_3}i_3;\\
\dot{U}_S=\left(Z_{R_7}+Z_{R_6}\right)i_8-Z_{R_7}i_6-Z_{R_6}i_7;\\
0=\left(Z_{R_3}+Z_{R_5}+Z_H\right)i_3+Z_{R_3}i_1-Z_{R_5}i_4;\\
0=\left(Z_{R_5}+Z_1+Z_{10}+Z_{13}\right)i_4-Z_{R_4}i_3-Z_1i_{13}-Z_9i_7-Z_{10}i_7+Z_{13}\left(I_4-i_{15}\right);\\
0=\left(Z_{R_4}+Z_2+Z_7+Z_{19}+Z_{18}\right)i_2+Z_{R_4}i_1-Z_2i_{13}+Z_7i_{17}+Z_{19}i_{10}-Z_{18}\left(I_3+i_{12}\right);\\
0=\left(Z_{R_7}+Z_{14}+Z_{12}\right)i_6-Z_{R_7}i_8-Z_{14}i_7-Z_{14}i_7-Z_{12}i_5;\\
0=\left(Z_8+Z_{10}+Z_{11}+Z_{14}+Z_{R_6}\right)i_7+Z_8i_{17}-Z_9i_4-Z_{10}i_4-Z_{11}i_5-Z_{14}i_6-Z_{R_6}i_8;\\
0=\left(Z_{16}+Z_{17}+Z_{18}\right)i_{12}+Z_{16}i_{10}+Z_{17}i_{11}+Z_{18}\left(I_3-i_2\right);\\
\dot{U}_S=\left(Z_{C_1}+Z_{R_8}\right)i_9+Z_{C_1}i_{10}+Z_{R_8}i_{11};\\
0=\left(Z_{C_1}+Z_{15}+Z_{16}+Z_{19}\right)i_{10}+Z_{C_1}i_9-Z_{15}i_{11}+Z_{16}i_{12}+Z_{19}i_2;\\
0=\left(Z_{R_8}+Z_{15}+Z_{17}\right)i_{11}+Z_{R_8}i_9-Z_{15}i_{10}+Z_{17}i_{10};\\
0=\left(Z_3+Z_4\right)i_{14}+Z_3i_{13}-Z_4i_{15}+Z_3\left(I_1+I_2\right)-Z_4\left(I_1+I_2\right);\\
0=\left(Z_1+Z_2+Z_3\right)i_{13}-Z_1i_4+Z_3\left(i_{14}+I_1\right)-Z_2i_2+Z_3I_2-Z_1\left(I_2+I_1\right)-Z_2\left(I_1+I_2\right);\\
0=\left(Z_6+Z_7+Z_8\right)i_{17}-Z_6i_{16}+Z_7i_2+Z_8i_7+Z_6\left(I_1+I_2\right)-Z_7\left(I_1+I_2\right)-Z_8\left(I_1+I_2\right),\\
0=\left(Z_4+Z_5\right)i_{15}-Z_4i_{14}-Z_5i_{16}+Z_4\left(I_1+I_2\right)-Z_5\left(I_1+I_2\right);\\
0=\left(Z_5+Z_6\right)i_{16}-Z_5i_{15}-Z_6i_{17}+Z_5\left(I_1+I_2\right)-Z_6\left(I_1+I_2\right);
\end{cases} \quad (1)$$

Having solved the system of equilibrium equations, we will find the total resistance at the electrodes of the transducer. Next, we will decompose the total resistance into real and imaginary components, determine the equivalent capacitance of the oscillating circuit, which depends on the magnetic induction.

Currents $I_{BS}$ (substrate-drain junction current) and $I_{BD}$ (substrate-drain junction current) in the linear mode if the condition is fulfilled $U_{ds}<(U_{gs}-U_T)$, are determined according to the expressions [19]

$$I_{bs}=I_{ss}(\exp U_{bs}/(NU_t)-1), \quad (2)$$

$$I_{bd}=I_{ss}(\exp U_{bd}/(NU_t)-1), \quad (3)$$

where $I_{ss}$ – the saturation current of the p-n junction of the substrate; $U_{bs}$ – substrate-source voltage; $U_{bd}$ – substrate-drain voltage; $N$ – coefficient of non-ideality of the substrate-flow transition; $U_t$ is the temperature potential of the p-n junction.

The static output characteristic of the MOSFET transistor in the linear mode is described by the expression [19]

$$I_{ds} = \frac{\mu \cdot C_0 \cdot W}{L}\left((U_{gs} - U_T)\cdot U_{ds} - \frac{U_{ds}^2}{2}\right), \quad (4)$$

where $L$ – channel length; $U_{gs}$ – gate-leakage voltage; $U_T$ is the threshold voltage; $W$ – channel width; $\mu$ – mobility of carriers in the channel; $C_0$ – specific capacity of the oxide; $U_{ds}$ – drain-leakage voltage; $U_T$ is the threshold voltage.

The threshold voltage of the MOSFET transistor for analytical models is described by the expression [22]

$$U_T = \varphi_{SiO_2} + 2\varphi_B - \frac{Q_S}{C_0} + \frac{1}{C_0}\sqrt{4_{\varepsilon_S}\cdot q \cdot N_A \cdot \varphi_B}\ , \quad (5)$$

where $Q_S$ – specific surface charge, $\Phi / м^2$; $\varepsilon_S$ – relative electrical permeability of the semiconductor; $N_A$ – concentration of impurities; $\varphi_B$ is the Fermi potential, which is described by the following expression [22]

$$\varphi_B = \pm kT / q \cdot \ln(N_A / n_i)\ . \quad (6)$$

The drain current in the saturation mode at $U_{ds} \geq (U_{gs} - U_T)$ is described by the formula [22]

$$I_{ds_{SAT}} = \frac{\mu \cdot C_0 \cdot W}{6L}((U_{ds_{SAT}} + 2\varphi_B)^2 + U_{gs}(U_{ds_{SAT}} + 2\varphi_B) - \\ -12\varphi_B(U_{gs} - \varphi_B - \frac{4}{3}K\varphi_B^{1/2})), \quad (7)$$

where

$$U_{ds_{SAT}} = U_{gs} - 2\varphi_B + K^2(1-(1+2U_{gs}/K^2)^{1/2}), \quad (8)$$

$$K = (\varepsilon_S q N_A / C_0)^{1/2}. \quad (9)$$

Drain-leakage resistance $R_{ds}$ in the linear region is determined by the formula [19]

$$R_{ds} = \frac{L}{W\mu C_0}(U_{gs} - U_T), \quad (10)$$

and in the saturation region

$$R_{ds} = \frac{12\left[L(U_d - U_{ds_{SAT}})^{1/2} - 2(\varepsilon_s / qN_a)^{1/2}(U_d - U_{ds_{SAT}})\right]}{W\mu C_0(2\varepsilon_s / qN_A)^{1/2}}\times \\ \times\frac{1}{(U_{ds_{SAT}} + 2\varphi_B)^2 + U_{gs}(U_{ds_{SAT}} + 2\varphi_B) - 12\varphi_B(U_{gs} - \varphi_B - 4/3K\varphi_B^{1/2})}, \quad (11)$$

where $U_d$ – voltage on the stock; $U_{ds_{SAT}}$ is the drain-drain voltage in the saturation mode.

Solving the system of equations 1 with the help of computer technology made it possible to obtain the theoretical dependence of the active and reactive components of the total resistance, as well as the transformation function and the sensitivity function,

which is a derivative of the transformation function. In fig. 5 shows the theoretical dependence of the active and reactive components of total resistance on magnetic induction.

Consider the scheme of Fig. 4 and the system of equilibrium equations (1). The Lyapunov function is a scalar function defined on the phase space of the system, which can be used to prove the stability of the equilibrium position [21].

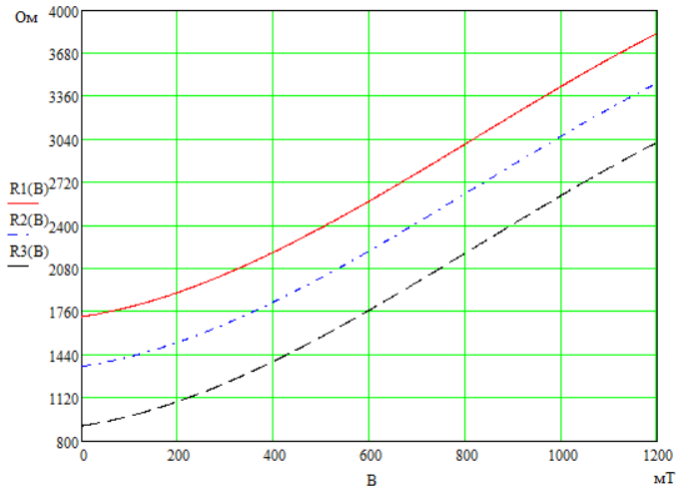


**Figure 5 – Dependence of the active component of the total resistance of the transducer on the induction of the magnetic field at different supply voltages: R1(B) – at $U_Ж$ = 6V; R2(B) - at $U_Ж$ = 5.5V; R3(B) - at $U_Ж$ = 5V**

Lyapunov functions allow establishing stability or instability of the system [21]. Based on the scheme (Fig. 4) in accordance with the Lyapunov method, the conversion function of the radio measuring transducer is determined, which represents the dependence of the generation frequency on the magnitude of the magnetic induction.

The analytical dependence of the transformation function has the form

$$F(B) = \frac{1}{2\pi}\sqrt{\frac{A_1^2 + R_B A_1 C_{DS2} - L_{екв} C_{DS2} + A_2}{2L_{екв} C_{DS2} A_1^2}}, \qquad (12)$$

where $A_1 = C_B(B)R_B(B)$, $A_2 = \sqrt{A_1^2 + R_H(B)A_1 C_{DS2} - L_{екв} C_{DS2})^2 + 4L_{екв} C_{DS2} A_1^2}$,

$C_H(B), R_H(B)$ is the equivalent capacity and resistance of the magnetosensitive element, $L_{екв}$ is the equivalent inductance of the frequency transducer, $C_{DS2}$ is the junction (drain-drain) capacitance of a two-gate transistor.

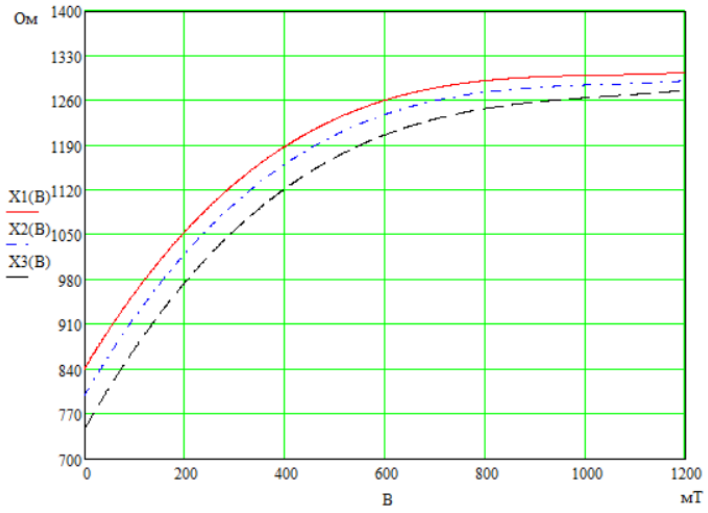


**Figure 6 – Dependence of the reactive component of the total resistance of the transducer on the induction of the magnetic field at different supply voltages: X1(B) – at $U_Ж$ = 6V; X2(B) - at $U_Ж$ = 5.5V; X3(B) - at $U_Ж$ = 5B**

The graphical dependence of the theoretical transformation function is presented in Fig. 7.

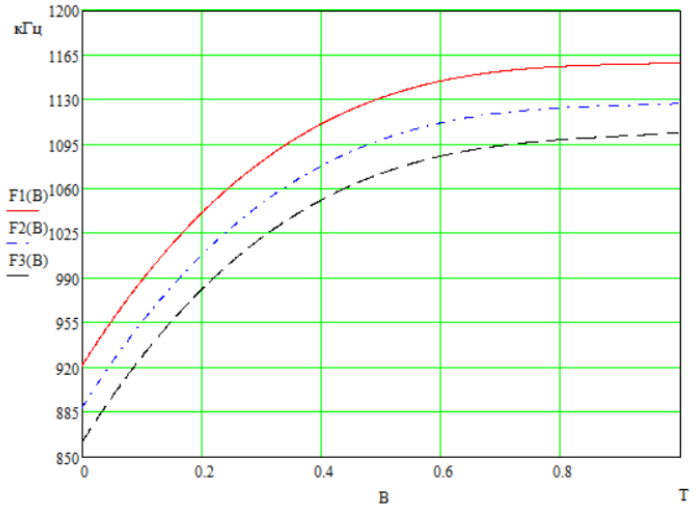


**Figure 7 – Graphs of the theoretical conversion function of the magnetic field transducer at different supply voltages: F1(B) – at $U_Ж$ = 6V; F2(B) - at $U_Ж$ = 5.5V; F3(B) - at $U_Ж$ = 5B**

The sensitivity of the transducer is determined as a derivative of the conversion function based on expression (13)

$$S(B) = \left| \frac{d(F(B))}{dB} \right|. \quad (13)$$

Thus, after performing the transformation, we get the equation

$$S_B^F = \frac{1}{\sqrt{8}}\left(\left(2C_H(B)R_H^2(B)\left(\frac{\partial C_H(B)}{\partial B}\right)+2C_H^2(B)R_H(B)\left(\frac{\partial R_H(B)}{\partial B}\right)+2R_H(B)C_H(B)C_{DS2}\times\right.\right.$$
$$\times\left(\frac{\partial R_H(B)}{\partial B}\right)+R_H^2(B)\left(\frac{\partial C_H(B)}{\partial B}\right)C_{DS2}+\frac{1}{2}\left(2\left(C_H^2(B)R_H^2(B)+C_H(B)R_H^2(B)C_{DS2}-L_{ekв}C_{DS2}\right)\times\right.$$
$$\times\left(2C_H(B)R_H^2(B)\left(\frac{\partial C_H(B)}{\partial B}\right)+2C_H^2(B)R_H(B)\left(\frac{\partial R_H(B)}{\partial B}\right)+2R_H(B)C_H(B)C_{DS2}\left(\frac{\partial R_H(B)}{\partial B}\right)+\right.$$
$$\left.+R_H^2(B)\left(\frac{\partial C_H(B)}{\partial B}\right)C_{DS2}\right)+8L_{ekв}C_{DS2}C_H(B)R_H^2(B)\left(\frac{\partial C_H(B)}{\partial B}\right)+8L_{ekв}C_{DS2}C_H^2(B)\times$$
$$\left.\left.\times R_H(B)\left(\frac{\partial R_H(B)}{\partial B}\right)\right)\Big/\left(\left(C_H^2(B)R_H^2(B)+C_H(B)R_H^2(B)C_{DS2}-L_{ekв}C_{DS2}\right)^2+4L_{ekв}C_{DS2}\times\right.$$
$$\times C_H^2(B)R_H^2(B))^{1/2}\Big)\Big/\Big(L_{ekв}C_{DS2}C_H^2(B)R_H^2(B))-2(C_H^2(B)R_H^2(B)+C_{DS2}C_H(B)R_H^2(B)-$$
$$-L_{ekв}C_{DS2}+\left((C_H^2(B)R_H^2(B)++C_{DS2}C_H(B)R_H^2(B)-L_{ekв}C_{DS2}\right)^2+4L_{ekв}C_{DS2}C_H^2(B)R_H^2(B))^{1/2}\Big)\times$$
$$\times\left(\frac{\partial C_H(B)}{\partial B}\right)\Big/\Big(L_{ekв}C_{DS2}C_H^3(B)R_H^2(B))-2(C_H^2(B)R_H^2(B)+C_{DS2}C_H(B)R_H^2(B)-L_{ekв}C_{DS2}+$$
$$+\left(C_H^2(B)R_H^2(B)+C_{DS2}C_H(B)R_H^2(B)-L_{ekв}C_{DS2}\right)^2+4L_{ekв}C_{DS2}C_H^2(B)R_H^2(B)\Big)^{1/2}\Big)\Big/\Big(L_{ekв}C_{DS2}\times$$
$$\times C_H^2(B)R_H^3(B))\Big)\Big/\Big(\Big(\Big(C_H^2(B)R_H^2(B)+C_{DS2}C_H(B)R_H^2(B)-L_{ekв}C_{DS2}+ \qquad (14)$$
$$+\left(\left(C_H^2(B)R_H^2(B)+C_{DS2}C_H(B)R_H^2(B)-L_{ekв}C_{DS2}\right)^2+\right.$$
$$\left.+4L_{ekв}C_{DS2}C_H^2(B)R_H^2(B))^{1/2}\right)\Big/\left(L_{ekв}C_{DS2}C_H^2(B)R_H^2(B)\right)^{1/2}.$$

The sensitivity graph is presented in Fig. 8. If we consider a magnetic field radio measuring device with such a radio measuring transducer, then since the output value of such a sensor is frequency, we can choose a digital frequency meter of instantaneous values as a means of measuring frequency. The conversion equation of this frequency meter is given in the form [20]:

$$N = \frac{T_X}{T_0} = T_X * f_0 = \frac{f_0}{f_X}.$$

By substituting expression (12) into the conversion equation of the frequency meter, we obtain the conversion equation of the entire device:

$$N = \frac{f_0}{F(B)}. \qquad (15)$$

As can be seen from the graph of fig. 8, the greatest sensitivity of the device lies in the range from 0...100 mT and is 300...600 Hz/mT. For the theoretical conversion function of the magnetic field induction radio measuring transducer at a supply voltage of 5V, we will linearize it. Let's divide the measurement range into three sub-ranges: the first 0...0.2 T; the second 0.2...0.8 T; the third 0.8...1 T.

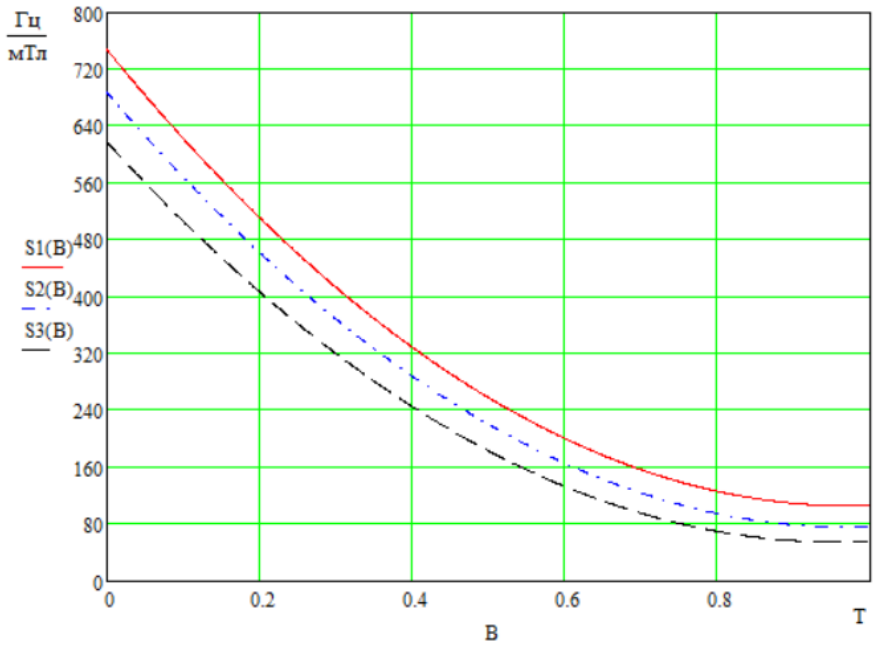


**Figure 8 – Theoretical dependence of sensitivity on the amount of magnetic induction at different supply voltages: S1(B) – at $U_{ж} = 6V$; S2(B) - at $U_{ж} = 5.5V$; S3(B) - at $U_{ж} = 5V$**

Using the mathematical package MathCad, we obtain the following expressions for the transformation function in subranges:

$$f_1(B) = 620B + 889\,;\; f_2(B) = 183B + 992\,;\; f_3(B) = 50B + 1085\,.$$

In fig. 9 shows the theoretical transformation function and approximated straight linessubranges.

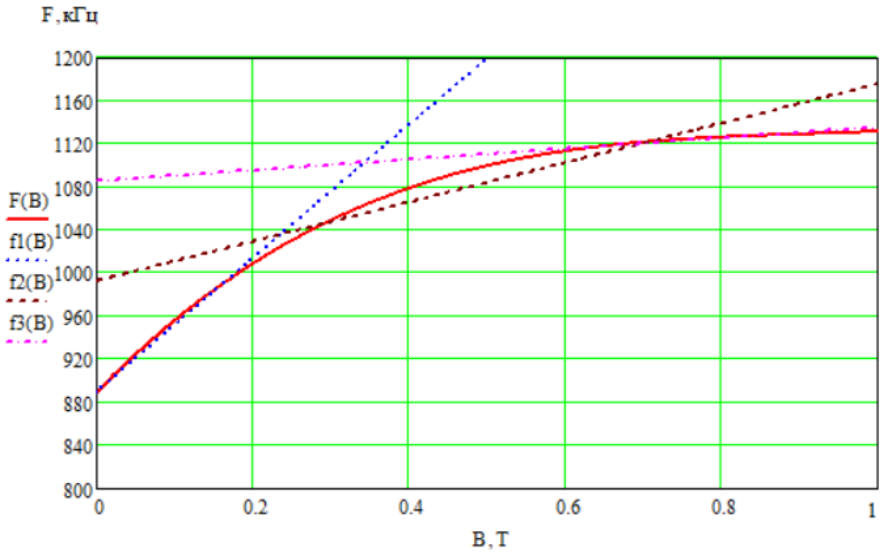


**Figure 9 – Graphs of the theoretical transformation function and its linearization lines in subranges**

Thus, upon linearization of the transformation function, we obtain the following sensitivity values in the subranges: 0-0.2 T: $S_1(B) = 620$ Hz/mT; 0.2-0.8 T: $S_2(B) = 183$ Hz/mT; 0.8-1 T: $S_3(B) = 50$ Hz/mT.

We will calculate the maximum nonlinearity error for each subrange using the formula:

$$\gamma_H = \frac{\Delta_{\max}}{|f_B - f_H|}, \quad (16)$$

where $\Delta_{\max}$ – the maximum deviation of the transformation function from the static characteristic, $f_B$, $f_H$ is the value of the transformation function at the end and at the beginning of the subrange.

By substituting numerical values, we get for eachsub-range:

$$\gamma_{H1} = \frac{1012-1007}{1012-890} = 0,041; \gamma_{H2} = \frac{1091-1076}{1138-1028} = 0,13; \gamma_{H3} = \frac{1128,5-1128}{1135-1125} = 0,05.$$

We can reduce the nonlinearity error by dividing it into a larger number of subranges. Using laboratory equipment, an experimental study of the functioning of the frequency transducer on bipolar and field-effect transistors without a magnetic sensor was conducted. For the demonstration, the static current-voltage characteristic was taken (Fig. 10) and the process of generating oscillations at different positions of the operating point on the falling section of the dynamic I-V characteristic was demonstrated (Fig. 11). When the operating point is placed on the growing section of the I-V, the generation of oscillations will be absent. Placing the operating point on the falling part of the I-V curve, we can get the so-called differential resistance in the oscillating circuit, which compensates for losses in it. In this case, oscillations with a certain frequency will be generated.

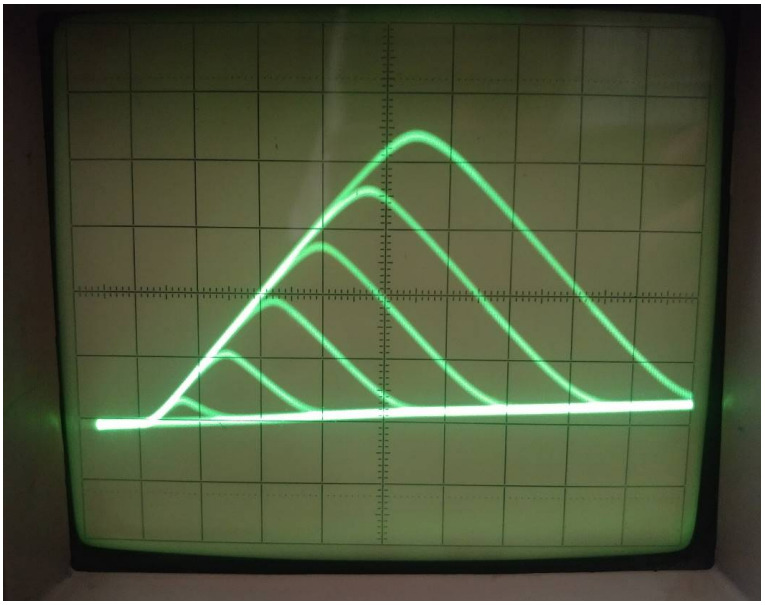

**Figure 10 – Static I-V of the frequency transducer on bipolar and field-effect transistors (one division on the vertical axis – 2mA, on the horizontal axis – 2V)**

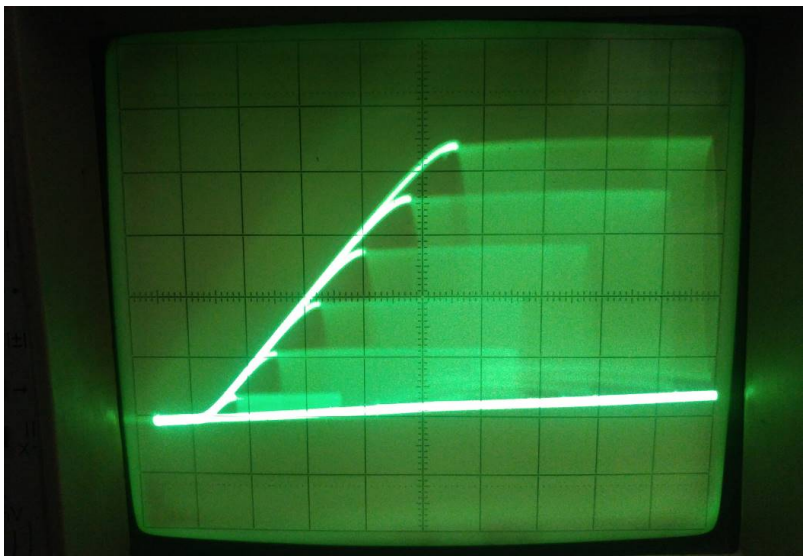

**Figure 11 – Dynamic I-V of the frequency transducer on bipolar and field-effect transistors (one division on the vertical axis – 2mA, on the horizontal axis – 2V)**

Having analyzed fig. 10 and fig. 11, the generation of oscillations can be fully confirmed. Moreover, the amplitude of oscillations is greater, the greater the supply voltage we apply to the frequency transducer. It is also necessary to take into account the fact that when the supply voltage increases, we change the position of the operating point on the I-V curve, and at a certain moment the generation of oscillations will disappear. Another factor in the development and improvement of frequency transducers for measuring devices is the introduction of their production in modern integrated technology, where in most cases a supply voltage of the order of 3 V or 5 V is used.

## 1.2. Mathematical model of radio-measuring frequency transducer based on DBMT and transistor structure on field-effect and bipolar transistors

The electric circuit of the radio measuring frequency transducer of the magnetic field is shown in fig. 12. The circuit consists of a double-collector magnetosensitive transistor (magnetic field sensor), a field-effect double-gate transistor and two bipolar transistors (they create an autogenerator device, the generation frequency of which varies depending on the voltage on the collector VT1).

Transistor VT4, capacitor C1 and resistor R11 form the active inductance of the frequency transducer. The implementation of active inductance can be performed in an integrated design, which corresponds to the modern technological process of manufacturing integrated microcircuits. Physical active inductance is a semiconductor device in which the necessary phase delay is created inside the device due to physical

processes in it. To simplify mathematical calculations, we replace in the scheme of Fig. 12 active inductance, which is formed by elements C1, VT4, R11, to inductance L1. We will get the resulting scheme of fig. 13.

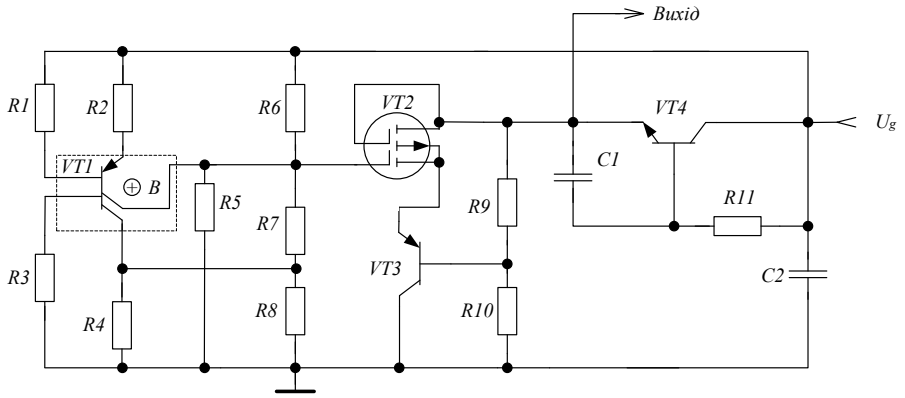


**Figure 12 – Electrical diagram of the magnetic field radio-measuring frequency transducer**

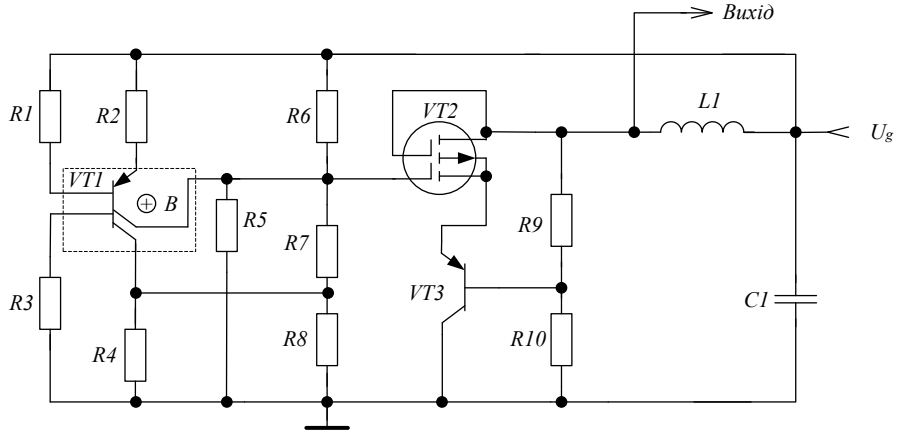


**Figure 13 – Electrical diagram of the radio-measuring frequency transducer of the magnetic field when replacing the active inductance**

The frequency transducer of the magnetic field based on two-collector and two-gate transistors with an active inductive element works as follows. At the electrodes of the collector of the bipolar transistor VT3 and the drain of the field-effect transistor VT2, there is a total resistance, the active component of which has a differential value, and the reactive component has a capacitive nature. Connecting the inductance (transistor analogue of the inductance based on bipolar transistor VT4 and the phase-shifting circuit C1–R11) to the drain of the two-gate field-effect transistor VT2 and the common bus through the blocking capacitance C1 creates an oscillating circuit in which energy losses are compensated by differential negative resistance. Resistors R9 and R10 provide the DC power mode of the circuit under study. During the action of a magnetic field on the two-collector magnetosensitive transistor VT1, the equivalent capacitance of the oscillating circuit changes, which causes a change in the resonant

frequency [13, 21, 23]. Resistors R9 and R10 provide the DC power supply mode (setting the required position of the operating point on the I-V curve) of the circuit under study. As a result of the influence of the magnetic field on the two-collector magnetosensitive transistor VT1, there is a change in the equivalent capacitance of the oscillating circuit, which in turn causes a change in the resonant frequency of the autogenerator. The equivalent circuit of the radio measuring frequency transducer of the magnetic field is presented in fig. 14. Resistors R9 and R10 provide the DC power supply mode (setting the required position of the operating point on the I-V curve) of the circuit under study. As a result of the influence of the magnetic field on the two-collector magnetosensitive transistor VT1, there is a change in the equivalent capacitance of the oscillating circuit, which in turn causes a change in the resonant frequency of the autogenerator. The equivalent circuit of the radio measuring frequency transducer of the magnetic field is presented in fig. 14. Resistors R9 and R10 provide the DC power supply mode (setting the required position of the operating point on the I-V curve) of the circuit under study. As a result of the influence of the magnetic field on the two-collector magnetosensitive transistor VT1, there is a change in the equivalent capacitance of the oscillating circuit, which in turn causes a change in the resonant frequency of the autogenerator. The equivalent circuit of the radio-measuring frequency transducer of the magnetic field is presented in fig. 14.

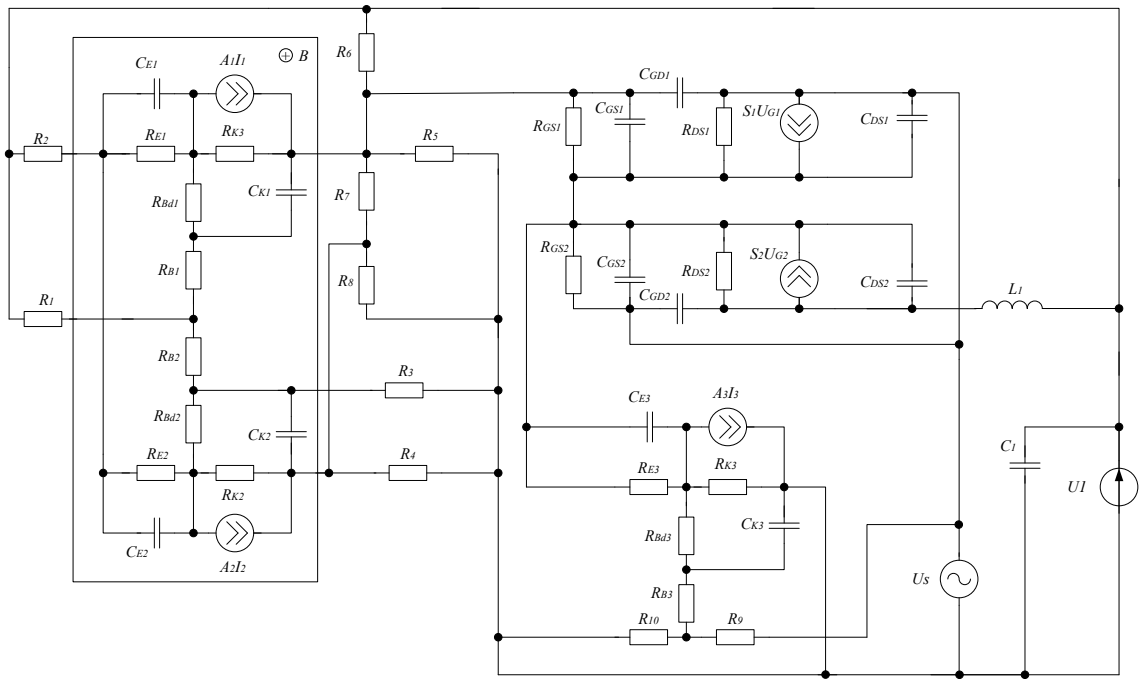


**Figure 14 – Equivalent circuit of the radio-measuring frequency transducer of the magnetic field with DBMT**

To simplify the calculations, let's convert the equivalent circuit of fig. 13 to the

circuit for alternating current, which is presented in fig. 14. For the scheme of fig. 14, we will perform the following actions: we will enter a complex form of recording for all elements of the diagram in Fig. 13; convert parallel and serial connections into one circuit element; denote the loop currents on the diagram.

Using the method of loop currents, we will create a system of equilibrium equations for this scheme. As a result, we will get the scheme of fig. 15.

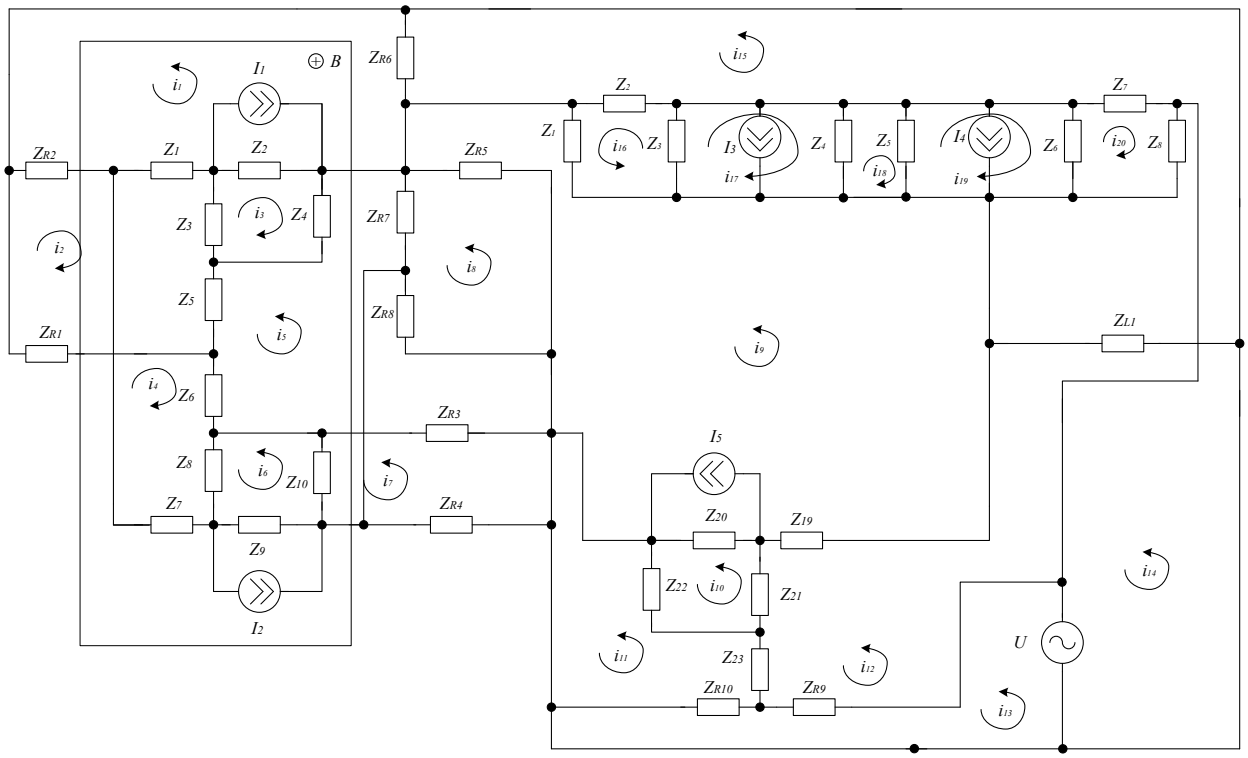


**Figure 15 – Transformed equivalent circuit of radio-measuring frequency transducer of magnetic field by alternating current**

In the scheme of fig. 15 elements are calculated as:

$$Z_{R_2} = R_2;\ Z_{R_1} = R_1;\ Z_{R_6} = R_6;\ Z_{R_5} = R_5;\ Z_{R_7} = R_7;\ Z_{R_8} = R_8;\ Z_{R_3} = R_3;\ Z_{R_4} = R_4;$$

$$Z_{R_{10}} = R_{10};\ Z_{R_9} = R_9;\ Z_1 = \frac{R_{E_1}}{1 + w^2 R_{E_1}^2 C_{E_1}^2} - j\frac{R_{E_1}^2 wC_{E_1}}{1 + wR_{E_1}^2 C_{E_1}^2};\ Z_2 = R_{k_1};\ Z_3 = R_{Bd_1};\ Z_4 = -\frac{j}{wC_{k_1}};$$

$$Z_5 = R_{B_1};\ Z_6 = R_{B_2};\ Z_8 = R_{Bd_2};\ Z_9 = R_{k_2};\ Z_{10} = -\frac{j}{wC_{k_2}};\ Z_7 = \frac{R_{E_2}}{1 + w^2 R_{E2}^2 C_{E2}^2} - j\frac{R_{E2}^2 wC_{E_2}}{1 + wR_{E2}^2 C_{E2}^2};$$

$$Z_{11} = \frac{R_{GS_1}}{1 + w^2 R_{GS_1}^2 C_{GS_1}^2} - j\frac{R_{GS_1}^2 wC_{GS_1}}{1 + wR_{GS_1}^2 C_{GS_1}^2};\ Z_{12} = -\frac{j}{wC_{GD_1}};\ Z_{13} = R_{DS_1};\ Z_{14} = -\frac{j}{wC_{DS_1}};$$

$$Z_{15} = -\frac{j}{wC_{DS_2}};\ Z_{16} = R_{DS_2};\ Z_{17} = -\frac{j}{wC_{GD_2}};\ Z_{18} = \frac{R_{GS2}}{1 + w^2 R_{GS2}^2 C_{GS2}^2} - j\frac{R_{GS2}^2 wC_{GS2}}{1 + wR_{GS2}^2 C_{GS2}^2};$$

$$Z_{19}=\frac{R_{E3}}{1+w^2R_{E3}^2C_{E3}^2}-j\frac{R_{E3}^2wC_{E3}}{1+wR_{E3}^2C_{E3}^2};\ Z_{20}=R_{k_3};\ Z_{21}=R_{Bd_3};\ Z_{22}=-\frac{j}{wC_{k_3}};\ Z_{23}=R_{B_3};\ Z_{L_1}=jwL_1;$$

Let's write down the system of Kirchhoff equations, according to the directions of the loop currents

$$\begin{cases}
0=\left(Z_2+Z_3+Z_4\right)i_3+Z_2(i_1-I_1)-Z_3i_2+Z_4i_5;\\
0=\left(Z_{R_2}+Z_1+Z_3+Z_5+Z_{R_1}\right)i_2+\left(Z_{R_2}+Z_1\right)i_1-Z_3i_3+Z_5\left(i_4+i_5\right);\\
\dot{U}=\left(Z_{R_{10}}+Z_{R_9}\right)i_{13}-Z_{R_{10}}i_{11}-Z_{R_9}i_{12};\\
0=\left(Z_1+Z_3+Z_5+Z_6+Z_7+Z_8\right)i_4-Z_3i_3+\left(i_1+i_2\right)Z_1+(Z_6+Z_6)i_5+\left(i_5+i_6\right)Z_8;\\
0=\left(Z_{R_2}+Z_1+Z_2+Z_{R_6}\right)i_1+Z_{R_2}i_2+Z_1i_2+Z_2\left(i_3-I_1\right)-Z_{R_6}i_{15}+Z_1i_4;\\
0=\left(Z_4+Z_5+Z_6+Z_8+Z_9+Z_{R_7}\right)i_5+Z_4i_3+\left(i_4+i_5\right)Z_5+Z_6i_4+\\
+\left(i_4+i_6\right)Z_8+Z_9\left(i_6+I_2\right)-Z_{R_7}i_8;\\
0=\left(Z_8+Z_9+Z_{10}\right)i_6+Z_8\left(i_5+i_4\right)+Z_9\left(i_5+I_2\right)-Z_{10}i_7;\\
0=\left(Z_{R_3}+Z_{R_4}+Z_{10}\right)i_7-Z_{10}i_6;\\
0=\left(Z_{11}+Z_{12}+Z_{13}\right)i_{16}-Z_{12}i_{15}-Z_{11}i_9+Z_{13}\left(I_3+I_4\right)+Z_{13}i_{17}-Z_{11}\left(I_3+I_4\right)-Z_{12}\left(I_3+I_4\right);\\
0=(Z_{R_5}+Z_{R_7}+Z_{R_8})i_8-Z_{R_7}i_5-Z_{R_5}i_9;\\
0=\left(Z_{22}+Z_{23}+Z_{R_{10}}\right)i_{11}-Z_{22}i_{10}-Z_{23}i_{12}-Z_{R_{10}}i_{13};\\
0=\left(Z_{R_5}+Z_{20}+Z_{19}+Z_{11}\right)i_9-Z_{R_5}i_8+Z_{20}\left(I_5-i_{10}\right)-Z_{19}i_{12}-Z_{11}i_{16};\\
0=\left(Z_{20}+Z_{21}+Z_{22}\right)i_{10}-Z_{22}i_{11}-Z_{21}i_{12}-Z_{20}\left(I_5+i_9\right);\\
0=\left(Z_{19}+Z_{21}+Z_{23}+Z_{R_9}+Z_{18}\right)i_{12}-Z_{19}i_9-Z_{21}i_{10}-Z_{23}i_{11}-Z_{R_9}i_{13}+Z_{18}i_{20};\\
\dot{U}=Z_{L_1}i_{14}-Z_{L_1}i_{15};\\
0=\left(Z_{R_6}+Z_{12}+Z_{17}+Z_{L_1}\right)i_{15}-Z_{R_6}i_1-Z_{12}i_{16}+Z_{17}i_{20}-Z_{L_1}i_{14};\\
0=\left(Z_{16}+Z_{17}+Z_{18}\right)i_{20}-Z_{16}i_{19}+Z_{18}i_{12}+Z_{17}i_{15}+Z_{16}\left(I_3+I_4\right)-Z_{17}\left(I_3+I_4\right)-Z_{18}\left(I_3+I_4\right);\\
0=\left(Z_{13}+Z_{14}\right)i_{17}+Z_{13}i_{16}-Z_{14}i_{18}+Z_{13}\left(I_3+I_4\right)-Z_{14}\left(I_3+I_4\right);\\
0=\left(Z_{15}+Z_{16}\right)i_{19}-Z_{15}i_{18}-Z_{16}i_{20}+Z_{15}\left(I_3+I_4\right)-Z_{16}\left(I_3+I_4\right);\\
0=\left(Z_{14}+Z_{15}\right)i_{18}-Z_{14}i_{17}-Z_{15}i_{19}+Z_{14}\left(I_3+I_4\right)-Z_{15}\left(I_3+I_4\right);
\end{cases}$$

(17)

In fig. 16 shows the theoretical dependence of the active component of total resistance on magnetic induction at three different supply voltages. In fig. 17 shows the theoretical dependence of the reactive component of total resistance on magnetic induction at three different transducer supply voltages.

Knowing the dependence of the elements of the equivalent circuit on the influence of the magnetic field, let's proceed to the definition of the conversion function and the sensitivity equation. The active inductance is a linear circuit [13], since the autogenerator operates in the low-frequency range in the linear mode of operation. Therefore, based on the method of algebraic linearization for the frequency of the first harmonic of the spectrum of generated electrical oscillations, the equivalent circuit of

the frequency transducer of the magnetic field will be linear with respect to the excitation action [94]. The obtained conversion function of the improved radio measuring transducer has the following form

$$F_0 = \frac{1}{2\pi}\sqrt{\frac{A_1 + \sqrt{A_1^2 + 4L_{екв}C_{GD}A_2^{\,2}}}{2L_{екв}C_{GD}A_2^{\,2}}}, \tag{18}$$

where $A_1 = L_{екв}C_{GD} - A_2^{\,2} - C_{GD}A_2R_B(B)$; $A_2 = C_B(B)R_B(B)$; $L_{ekv}$ – equivalent inductance of the transistor analogue of the inductance; $C_B(B)$ is the equivalent capacitance of the base region of a bipolar two-collector magnetotransistor; $R_B(B)$ – equivalent resistance of the base region of a bipolar two-collector magnetotransistor; $C_{GD}$ is the capacitance of the gate-drain region of the MOSFET transistor.

If we consider a radio-measuring device of the magnetic field with such a radio-measuring transducer, then substituting the expression (18) in (13), we get the conversion equation of the entire device with the following frequency transducer:

$$N = \frac{f_0}{\frac{1}{2\pi}\sqrt{\frac{A_1 + \sqrt{A_1^2 + 4L_{екв}C_{GD}A_2^{\,2}}}{2L_{екв}C_{GD}A_2^{\,2}}}}. \tag{19}$$

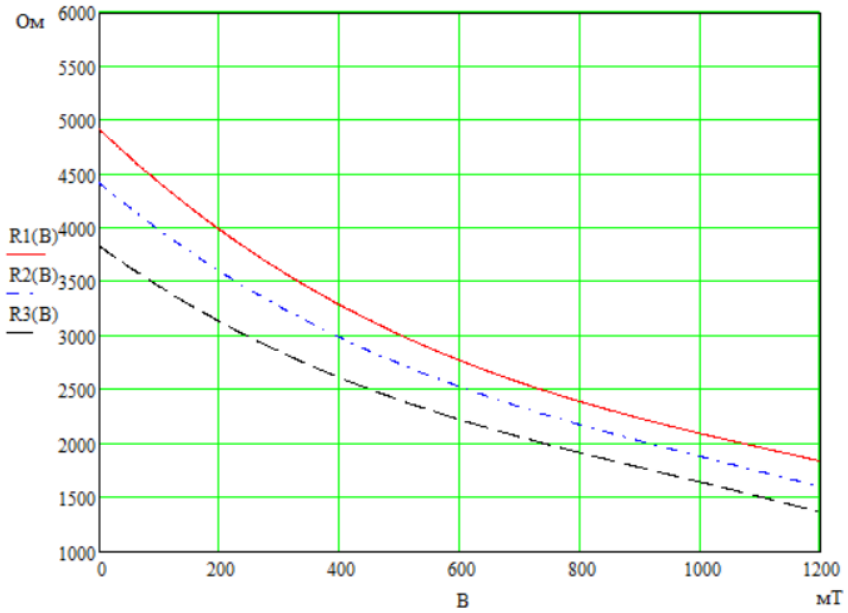


**Figure 16 – Dependencies of the active component of the total resistance of the transducer on magnetic induction for three different supply voltages: R1(B) – at $U_Ж = 6V$; R2(B) - at $U_Ж = 5.5V$; R3(B) - at $U_Ж = 5V$**

The graph of the conversion function of the developed radio measuring transducer is shown in Fig. 18.

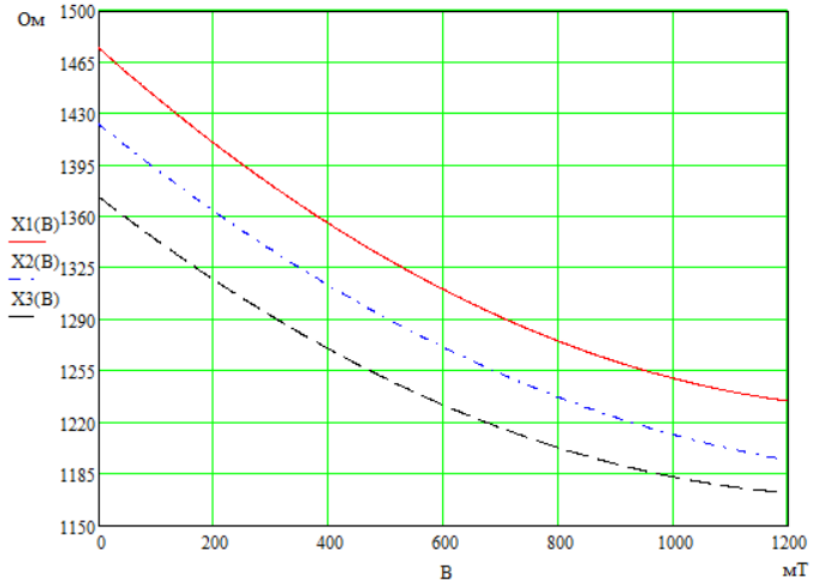


**Figure 17 – Dependencies of the reactive component of the total resistance of the transducer on magnetic induction for three supply voltages: X1(B) – at $U_{ж} = 6$V; X2(B) – at $U_{ж} = 5.5$V; X3(B) - at $U_{ж} = 5$V**

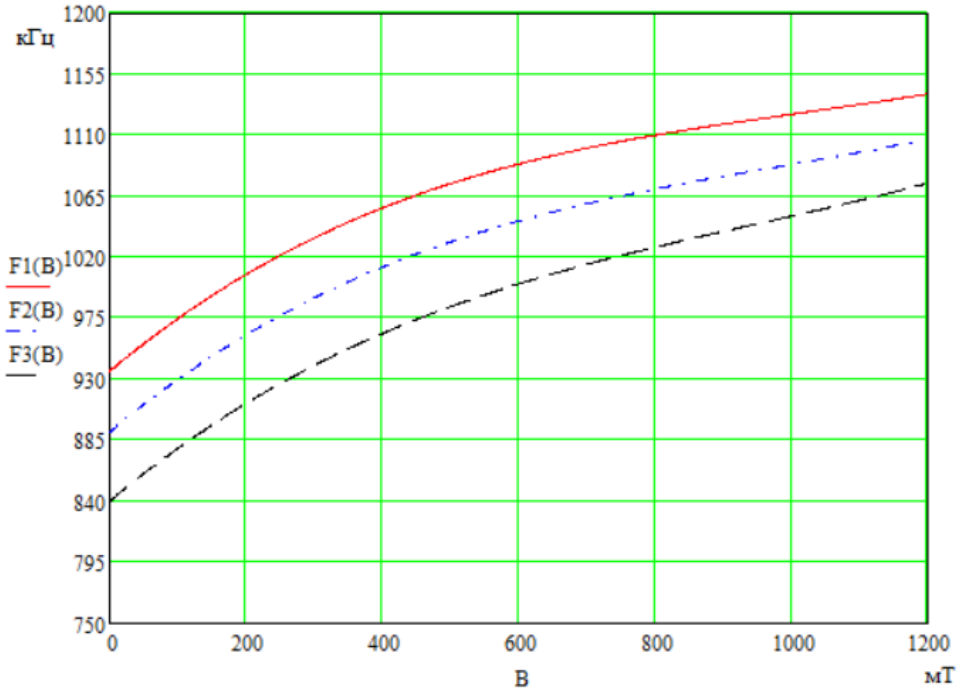


**Figure 18 – Dependence of the generation frequency on the induction of the magnetic field of the radio-measuring transducer at different supply voltages: F1(B) - at $U_{ж} = 6$ V; F2(B) - at $U_{ж} = 5.5$V; F3(B) - at $U_{ж} = 5$V**

The sensitivity function is determined on the basis of the transformation equation (17) and has the following form

$$S_B^{F_0} = -0.0198\left(-2C_B(B)R_B^3(B)C_{GD}\left(\frac{\partial C_B(B)}{\partial B}\right)\sqrt{A_1+2A_2} - 2C_B^2(B)R_B^3(B)\times\right.$$
$$\times\left(\frac{\partial C_B(B)}{\partial B}\right) - 2C_B^3(B)R_B^2(B)\left(\frac{\partial R_B(B)}{\partial B}\right) - 3C_B(B)R_B^3(B)C_{GD}\left(\frac{\partial C_B(B)}{\partial B}\right) -$$
$$-2C_{GD}C_B^2(B)R_B^2(B)\left(\frac{\partial R_B(B)}{\partial B}\right) + 8C_B^2(B)R_B^3(B)LC_{GD}\left(\frac{\partial C_B(B)}{\partial B}\right) + 8LC_{GD}C_B^2(B)\times$$
$$\times R_B^2(B)\left(\frac{\partial R_B(B)}{\partial B}\right) + 4LC_{GD}R_B(B)\left(\frac{\partial C_B(B)}{\partial B}\right)\sqrt{A_1+2A_2} + 4R_B(B)\times$$
$$\times\left(\frac{\partial C_B(B)}{\partial B}\right)LC_{GD} + 4C_B(B)LC_{GD}\left(\frac{\partial R_B(B)}{\partial B}\right)\sqrt{A_1+2A_2} + 4LC_{GD}C_B(B)\times$$
$$\left.\times\left(\frac{\partial R_B(B)}{\partial B}\right)\right)\Big/\left(\left(2\sqrt{A_1+\sqrt{A_1+2A_2}}\Big/A_2\right)LC_{GD}C_B^3(B)R_B^3(B)\sqrt{A_1+2A_2}\right) \quad (20)$$

where $A_2 = 2LC_{GD}(C_B(B)R_B(B))^2$.

The graph of the measurement sensitivity function is shown in Fig. 19.

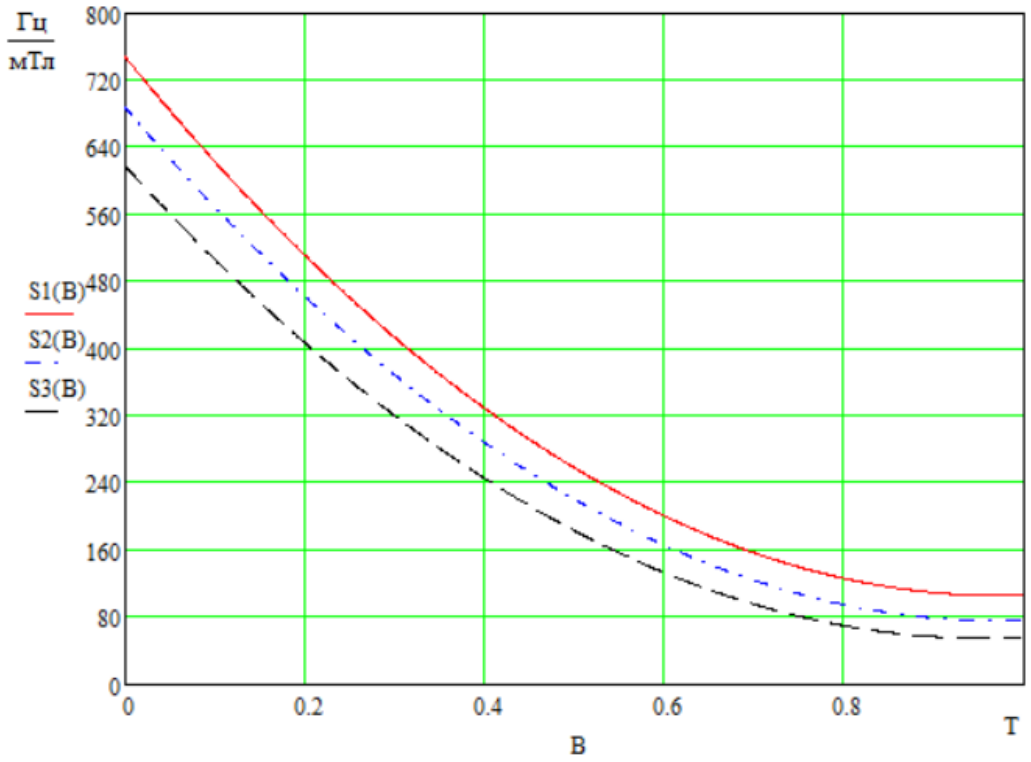


**Figure 19 – The graph of the change in sensitivity from the value of the magnetic induction of a frequency transducer based on a double-collector magnetotransistor with an active inductive element at different supply voltages: S1(B) - at $U_Ж$ = 6V; S2(B) - at $U_Ж$ = 5.5V; S3(B) - at $U_Ж$ = 5V**

As can be seen from fig. 19, the frequency transducer of the magnetic field based on two-collector, two-gate and two bipolar transistors has the highest sensitivity in the range from 0 to 200 mT and is 240...405 Hz/mT at a supply voltage of 5.5V.

For the theoretical conversion function of the radio-measuring magnetic field induction transducer at a supply voltage of 5V, we will linearize it. Let's divide the measurement range into two sub-ranges: from 0 to 0.3 T; 0.3 – 1 T. Using the MathCad mathematical package, we obtain the following expressions for the transformation function in the subranges:

$$f_1(B) = 0,35B + 840\,;\; f_2(B) = 0,15B + 905\,.$$

In fig. 20 shows the theoretical transformation function and approximate lines in the subbands.

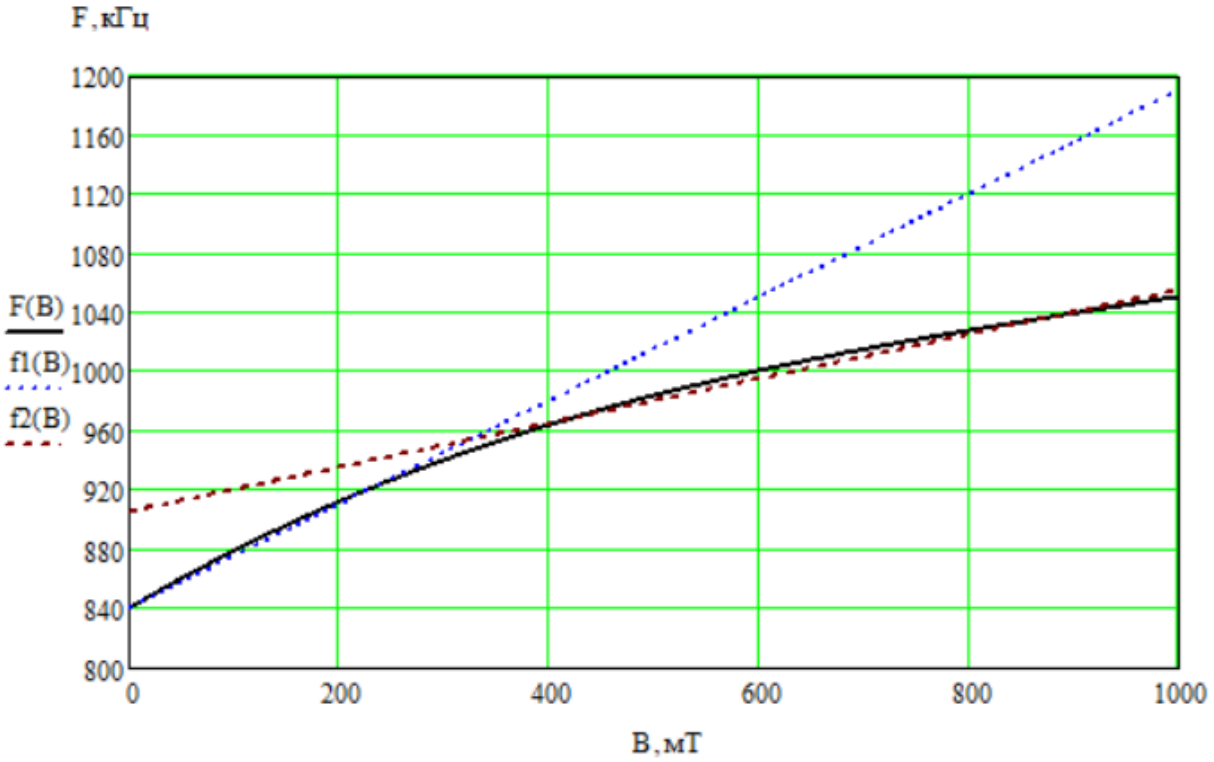


**Figure 20 – Graphs of the theoretical transformation function and direct lines of its linearization in subranges**

Thus, upon linearization of the transformation function, we obtain the following sensitivity values in the subbands:

$$\text{0-0.3 T: } S_1(B) = 350\text{Hz/mTl};\ \text{0.3-1 T: } S_2(B) = 150\text{Hz/mTl}.$$

We will calculate the maximum nonlinearity error for each sub-range according to formula (14).

By substituting numerical values, we get for eachsub-range:

$$\gamma_{H1} = \frac{942 - 940}{949 - 839} = 0,018\,;\; \gamma_{H2} = \frac{1007 - 1002}{1055 - 950} = 0,047\,.$$

We can reduce the nonlinearity error by dividing it into a larger number of subranges. But in each specific case, it is necessary to determine whether it is appropriate to do this.

As we can see from the calculations, that for this variant, even when divided into only two sub-bands, we get a smaller nonlinearity error compared to the previous radio-measuring frequency transducer.

The sensitivity of this version of the transducer decreased almost twice with magnetic induction to 300 mT.

## 1.3. Mathematical model of radio-measuring frequency transducer based on DBMT and transistor structure on bipolar transistors

The scheme of the radio-measuring frequency transducer of the magnetic field is shown in Fig. 21. two-collector bipolar magnetotransistor VT1 is used as a magnetically sensitive sensor. VT2, VT3 and VT4 implement an electrical oscillation generator, in which the oscillating circuit is formed by the capacitive component of total resistance with a negative value of the active component at the collector-collector electrodes of bipolar transistors VT2 and VT3 and the inductive component of total resistance at the emitter-collector electrodes of bipolar transistor VT4. As a result, we have that when a magnetic field is applied to a two-collector bipolar magnetotransistor VT1, an informative amplitude signal arises that changes the equivalent capacitance of the oscillator, which in turn leads to a change in the generation frequency of the oscillator, which significantly increases the sensitivity of the transducer.

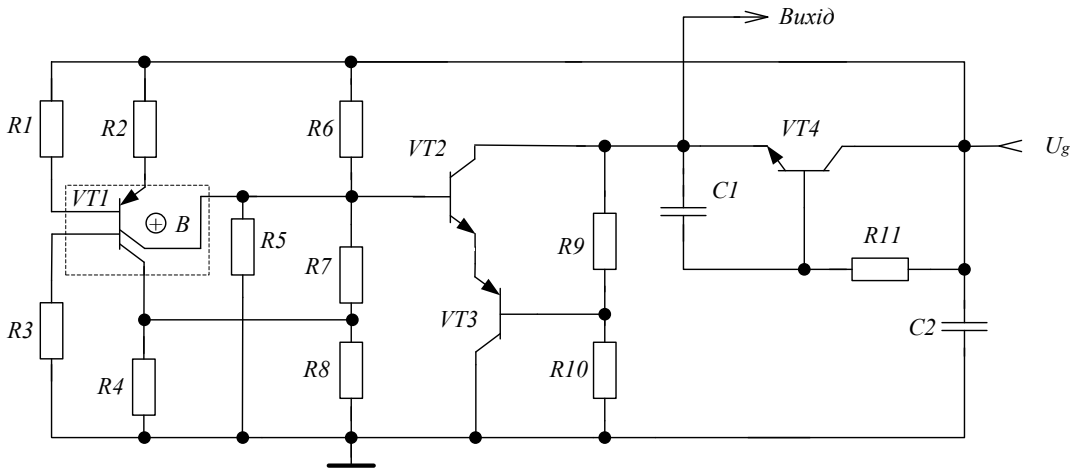


**Figure 21 – Electrical diagram of the radio-measuring frequency transducer on a bipolar magnetosensitive structure with an active inductive element**

To simplify mathematical calculations, we replace in the scheme of Fig. 21 scheme of active inductance on inductance L1. We will get the resulting scheme of fig. 22.

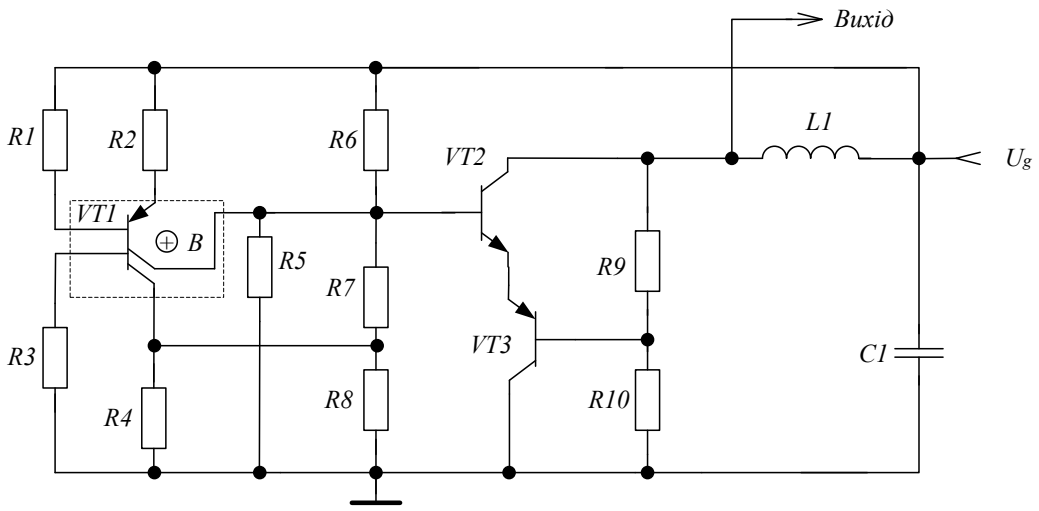


**Figure 22 – Electrical diagram of the radio measuring frequency transducer on a bipolar magnetosensitive structure with a passive inductive element**

In order to create a mathematical model of this version of the radio-measuring magnetic field transducer, we need to convert this scheme into an equivalent one, with further description of it through a system of equilibrium equations. So, let's replace the transistors with their equivalent circuits and get an equivalent circuit.

The equivalent circuit of the radio measuring frequency transducer of the magnetic field is presented in fig. 21. It is a linear circuit, since the autogenerator works in the low-frequency region in a linear mode of operation. Therefore, based on the method of algebraic linearization for the frequency of the first harmonic of the spectrum of generated electrical oscillations, the equivalent circuit of the frequency transducer of the magnetic field will be linear with respect to the exciting action.

For the scheme of fig. 23, we will perform the following actions: we will enter a complex form of record for all elements of the diagram in Fig. 23; convert parallel and serial connections into one circuit element; denote the loop currents on the diagram.

Using the method of loop currents, we will create a system of equilibrium equations for this circuit. As a result, we will get the scheme of fig. 24. The complex form of recording for all elements of an electric circuit can be used to calculate alternating current circuits. With a complex form of recording, well-known methods of calculating direct current circuits, such as the method of loop currents, the method of nodal potentials, the conversion method, and others, can also be used to calculate alternating current circuits.

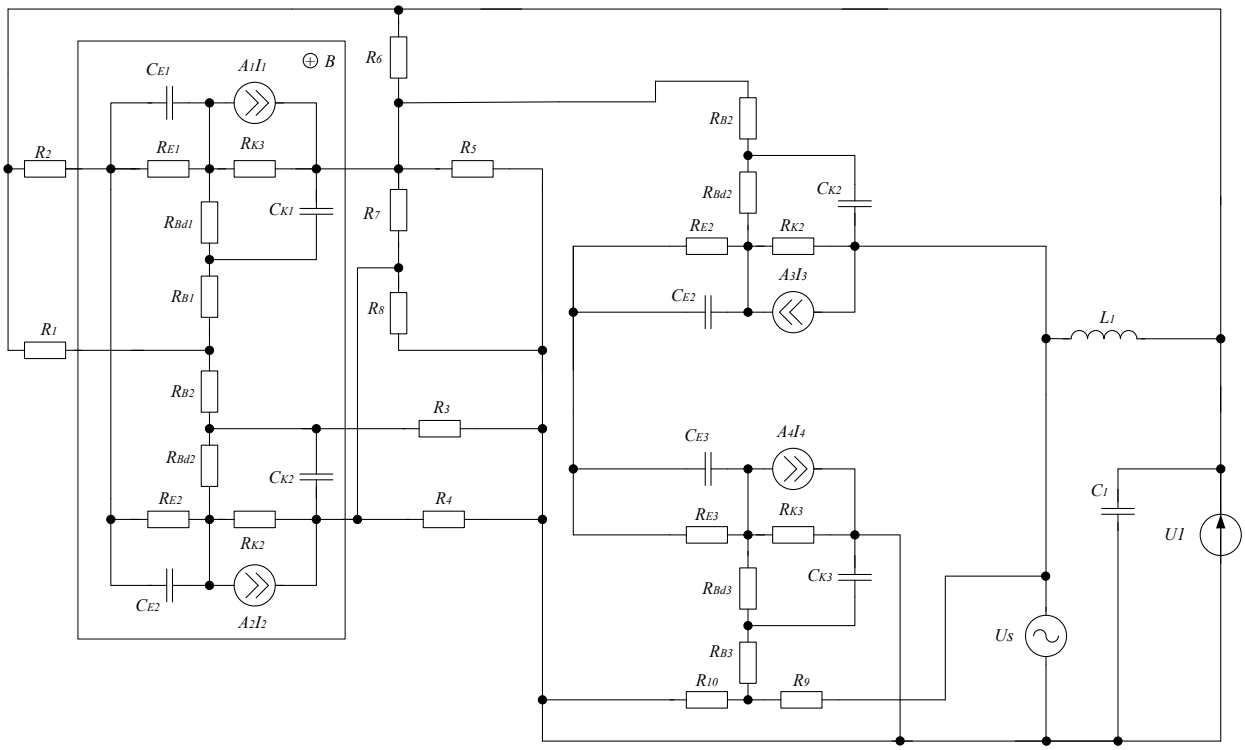


**Figure 23 – Equivalent circuit of the radio measuring frequency transducer of the magnetic field with DBMT**

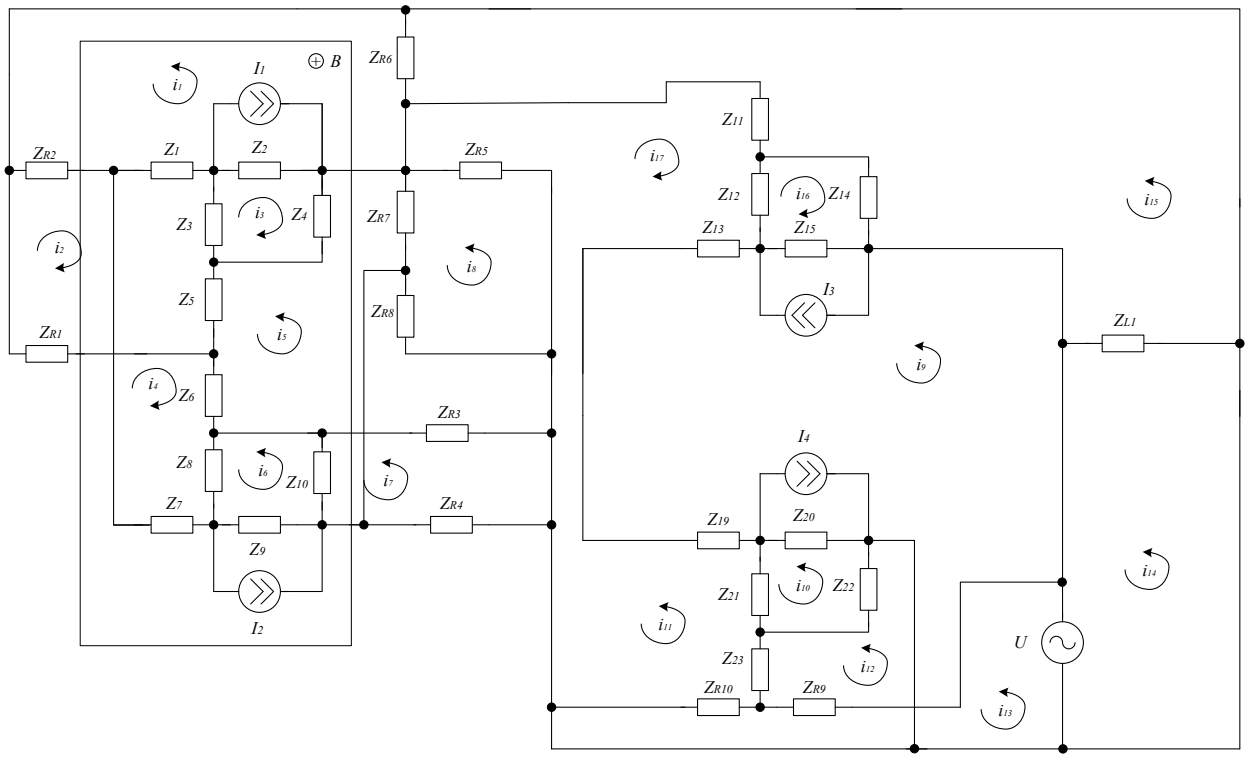


**Figure 24 – Transformed non-linear equivalent circuit of the magnetic induction frequency transducer**

In the scheme of fig. 24 elements are calculated as:

$$Z_{R_2} = R_2\,;\, Z_{R_1} = R_1\,;\, Z_{R_6} = R_6\,;\, Z_{R_5} = R_5\,;\, Z_{R_7} = R_7\,;\, Z_{R_8} = R_8\,;\, Z_{R_3} = R_3\,;\, Z_{R_4} = R_4\,;\, Z_{R_{10}} = R_{10}\,;\, Z_{R_9} = R_9\,;$$

$$Z_1 = \frac{R_{E_1}}{1+w^2R_{E_1}^2C_{E_1}^2} - j\frac{R_{E_1}^2wC_{E_1}}{1+wR_{E_1}^2C_{E_1}^2}; Z_2 = R_{k_1}; Z_3 = R_{Bd_1}; Z_4 = -\frac{j}{wC_{k_1}}; Z_5 = R_{B_1}; Z_6 = R_{B_2}; Z_8 = R_{Bd_2};$$

$$Z_9 = R_{k_2}; Z_{10} = -\frac{j}{wC_{k_2}}; Z_7 = \frac{R_{E_2}}{1+w^2R_{E2}^2C_{E2}^2} - j\frac{R_{E2}^2wC_{E_2}}{1+wR_{E2}^2C_{E2}^2}; Z_{11} = \frac{R_{GS_1}}{1+w^2R_{GS_1}^2C_{GS_1}^2} - j\frac{R_{GS_1}^2wC_{GS_1}}{1+wR_{GS_1}^2C_{GS_1}^2};$$

$$Z_{12} = R_{Bd_2}; Z_{13} = \frac{R_{E2}}{1+w^2R_{E2}^2C_{E2}^2} - j\frac{R_{E2}^2wC_{E2}}{1+wR_{E2}^2C_{E2}^2}; Z_{14} = -\frac{j}{wC_{k_2}}; Z_{15} = R_{k_2};$$

$$Z_{19} = \frac{R_{E3}}{1+w^2R_{E3}^2C_{E3}^2} - j\frac{R_{E3}^2wC_{E3}}{1+wR_{E3}^2C_{E3}^2}; Z_{20} = R_{k_3}; Z_{21} = R_{Bd_3}; Z_{22} = -\frac{j}{wC_{k_3}}; Z_{23} = R_{B_3}; Z_{L_1} = jwL_1.$$

We take the method of contour currents as the basis of the study. We determine the independent contours of the transformed equivalent circuit in fig. 22 and mark in these contours the directions of the corresponding contour currents. The system of Kirchhoff equations, according to the scheme, has the form (21).

$$\begin{cases}
0 = \left(Z_{R_2} + Z_1 + Z_2 + Z_{R_6}\right)i_1 + Z_{R_2}i_2 + Z_1i_2 + Z_2\left(i_3 - I_1\right) - Z_{R_6}i_{15} + Z_1i_4; \\
0 = \left(Z_{11} + Z_{12} + Z_{13}\right)i_{17} + Z_{11}i_{15} + Z_{13}i_9 + Z_{13}\left(I_3 + I_4\right) + Z_{13}i_{17} \\
0 = \left(Z_2 + Z_3 + Z_4\right)i_3 + Z_2(i_1 - I_1) - Z_3i_2 + Z_4i_5; \\
0 = \left(Z_1 + Z_3 + Z_5 + Z_6 + Z_7 + Z_8\right)i_4 - Z_3i_3 + \left(i_1 + i_2\right)Z_1 + (Z_6 + Z_6)i_5 + \left(i_5 + i_6\right)Z_8; \\
\dot{U} = \left(Z_{R_{10}} + Z_{R_9}\right)i_{13} - Z_{R_{10}}i_{11} - Z_{R_9}i_{12}; \\
0 = \left(Z_4 + Z_5 + Z_6 + Z_8 + Z_9 + Z_{R_7}\right)i_5 + Z_4i_3 + \left(i_4 + i_5\right)Z_5 + Z_6i_4 + \\
+ \left(i_4 + i_6\right)Z_8 + Z_9\left(i_6 + I_2\right) - Z_{R_7}i_8; \\
0 = \left(Z_8 + Z_9 + Z_{10}\right)i_6 + Z_8\left(i_5 + i_4\right) + Z_9\left(i_5 + I_2\right) - Z_{10}i_7; \\
0 = \left(Z_{R_3} + Z_{R_4} + Z_{10}\right)i_7 - Z_{10}i_6; \\
0 = (Z_{R_5} + Z_{R_7} + Z_{R_8})i_8 - Z_{R_7}i_5 - Z_{R_5}i_9; \\
\dot{U} = Z_{L_1}i_{14} - Z_{L_1}i_{15}; \\
0 = \left(Z_{R_5} + Z_{20} + Z_{19} + Z_{11}\right)i_9 - Z_{R_5}i_8 + Z_{20}\left(I_5 - i_{10}\right) - Z_{19}i_{12} - Z_{11}i_{16}; \\
0 = \left(Z_{20} + Z_{21} + Z_{22}\right)i_{10} - Z_{22}i_{11} - Z_{21}i_{12} - Z_{20}\left(I_5 + i_9\right); \\
0 = \left(Z_{22} + Z_{23} + Z_{R_{10}}\right)i_{11} - Z_{22}i_{10} - Z_{23}i_{12} - Z_{R_{10}}i_{13}; \\
0 = \left(Z_{19} + Z_{21} + Z_{23} + Z_{R_9}\right)i_{12} - Z_{19}i_9 - Z_{21}i_{10} - Z_{23}i_{11} - Z_{R_9}i_{13} + Z_{18}i_{20}; \\
0 = \left(Z_{R_2} + Z_1 + Z_3 + Z_5 + Z_{R_1}\right)i_2 + \left(Z_{R_2} + Z_1\right)i_1 - Z_3i_3 + Z_5\left(i_4 + i_5\right); \\
0 = \left(Z_{R_6} + Z_{11} + Z_{14} + Z_{L_1}\right)i_{15} - Z_{R_6}i_1 + Z_{14}i_{16} + Z_{11}i_{17} - Z_{L_1}i_{14}; \\
0 = \left(Z_{13} + Z_{14}\right)i_{17} + Z_{13}i_{16} - Z_{14}i_{18} + Z_{13}\left(I_3 + I_4\right) - Z_{14}\left(I_3 + I_4\right);
\end{cases} \quad (21)$$

Solving this system using a computer numerical method, the value of the total

resistance was obtained. In fig. 25 shows the theoretical dependence of the active component of total resistance on magnetic induction at three different supply voltages: R1(B) – at $U_{ж} = 5V$; R2(B) – at $U_{ж} = 4V$; R3(B) – at $U_{ж} = 3V$. In fig. 26 shows the theoretical dependence of the reactive component of total resistance on magnetic induction at three different supply voltages: X1(B) – at $U_{ж} = 5V$; X2(B) - at $U_{ж} = 4V$; X3(B) – at $U_{ж} = 3V$.

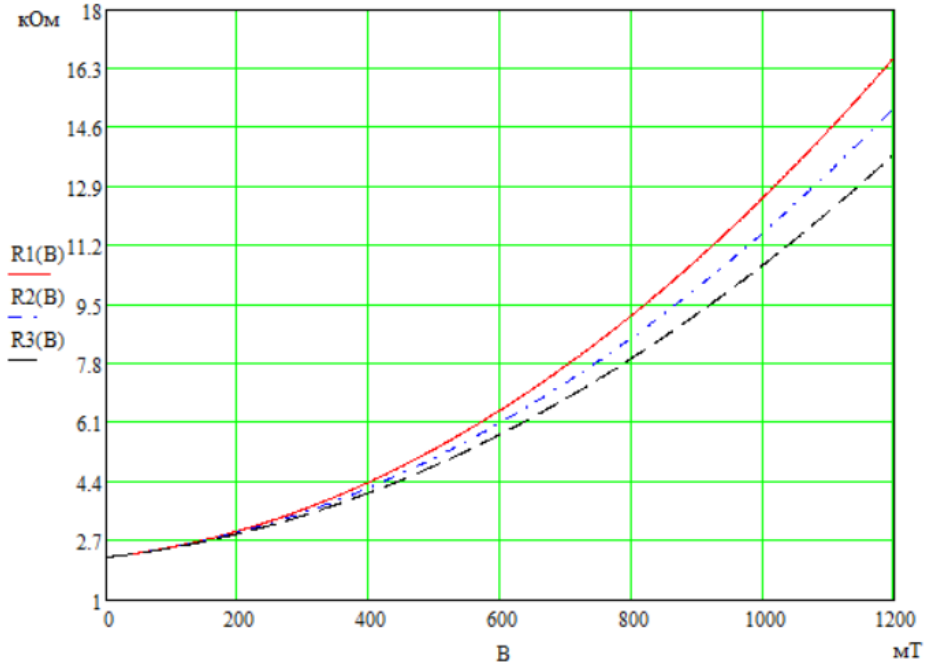


**Figure 25 – Dependences of the active component of the total resistance on the induction of the magnetic field for three different transducer supply voltages**

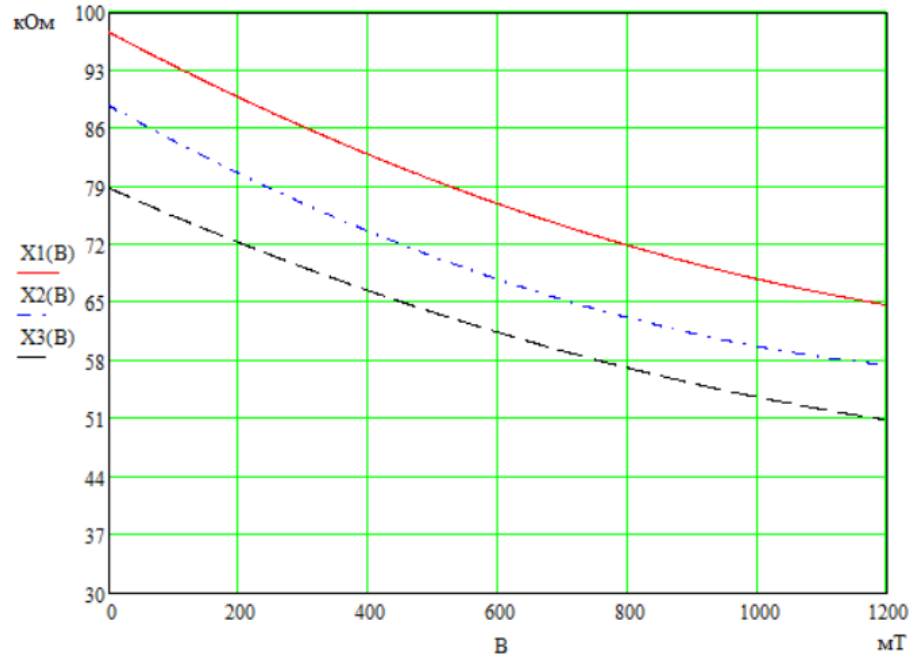


**Figure 26 – Dependencies of the reactive component of the total resistance from magnetic field induction for three transducer supply voltages**

The influence of the magnetic field on the equivalent capacitance and inductance of the oscillating circuit is transmitted through a change in the parameters of the elements of the equivalent circuit, so the transformation function is described by the equation

$$F_0 = \frac{1}{2\pi}\sqrt{\frac{-(A_1 - A_3) + \sqrt{(A_1 - A_3)^2 + 8(C_e + C_b)LC_bC_eA_2^2}}{2L_{екв}C_bC_eA_2^2}}, \quad (22)$$

where $A_1 = L_{екв}C_bC_e - (C_e + C_b)A_2^2$, $A_2 = C_B(B)R_B(B)$, $A_3 = R_B^2(B)C_B(B)C_eC_b$,

$L_{екв}$, $C_b$, $C_e$ – equivalent inductance, base and emitter capacitance.

The graphic dependence of the conversion function of the transducer is presented in Fig. 27.

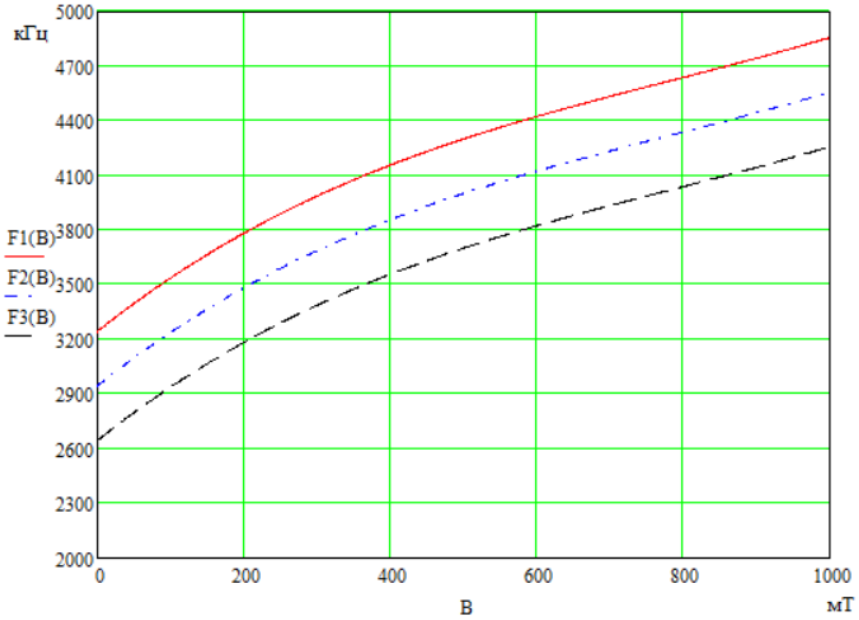


**Figure 27 – Graph of the conversion function for a radio measuring transducer at three supply voltages: F1(B) – at $U_Ж$ = 5V; F2(B) - at $U_Ж$ = 4V; F3(B) - at $U_Ж$ = 3V**

The sensitivity of the transducer is determined on the basis of expression (21) and is described by the equation

$$S_B^{F_0} = \frac{1}{8}\left(2(C_e + C_bC_3^2(B)R_3(B)\left(\frac{\partial R_3(B)}{\partial B}\right) + 2R_3(B)C_3(B)C_eC_b\left(\frac{\partial R_3(B)}{\partial B}\right) + \right.$$
$$+\frac{1}{2}\left(2(A_1 - D_1)\left(-2(C_e + C_b)C_3^2(B)R_3(B)\left(\frac{\partial R_3(B)}{\partial B}\right) - 2R_3(B)C_3(B)C_eC_b\left(\frac{\partial R_3(B)}{\partial B}\right)\right) + \quad (23)$$
$$\left.+24(C_e + C_b)LC_eC_bC_3^2(B)R_3(B)\left(\frac{\partial R_3(B)}{\partial B}\right)\right)\Big/\sqrt{(A_1 - D_1)^2 + 12Y_1} - \Big)\Big/\pi LC_eC_b \times$$
$$\times C_3^2(B)R_3(B) - \frac{1}{4}\left(\left(-A_1 + D_1 + \sqrt{(A_1 - D_1)^2 + 12Y_1}\right)\left(\frac{\partial R_3(B)}{\partial B}\right)\right)\Big/\left(\pi LC_eC_bC_3^2(B)R_3^3(B)\right),$$

where $Y_1 = (C_e + C_b)LC_eC_bC_3^2(B)R_3^2(B)$.

The dependence of sensitivity on magnetic field induction is shown in Fig. 28.

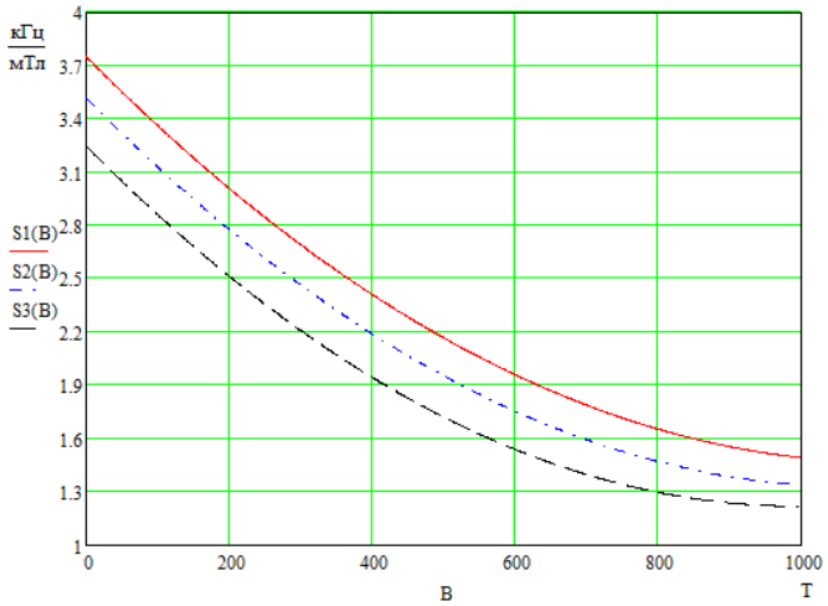


**Figure 28 – Dependence of the sensitivity of the transducer on magnetic induction at three supply voltages: S1(B) – at $U_{ж}$ = 5V; S2(B) – at $U_{ж}$ = 4V; S3(B) – at $U_{ж}$ = 3V**

If we consider a radio-measuring device of the magnetic field with such a radio-measuring transducer, then substituting the expression (22) in (15), we get the conversion equation of the entire device with the following frequency transducer:

$$N = \frac{f_0}{\frac{1}{2\pi}\sqrt{\frac{-(A_1 - A_3) + \sqrt{(A_1 - A_3)^2 + 8(C_e + C_b)LC_bC_eA_2^2}}{2L_{екв}C_bC_eA_2^2}}}. \qquad (24)$$

Analysis of the graphs of fig. 28 shows that as the value of magnetic field induction increases, the sensitivity of the radio measuring transducer decreases. In the range from 0 to 200 mT, the sensitivity plots are close to linear. And in this range, the measurement sensitivity of the radio measuring frequency transducer of the device varies from 1.8 kHz/mT to 3.3 kHz/mT. An experimental study of the functioning of the frequency transducer on bipolar transistors without a magnetic sensor was carried out. For demonstration, the current-voltage characteristic was taken at different supply voltages (Fig. 29).

From fig. 29, it can be seen that the I-V characteristics of the transistor structure have both a rising and a falling section. Placing the operating point on the falling part of the I-V, we can get the generation of oscillations (Fig. 30).

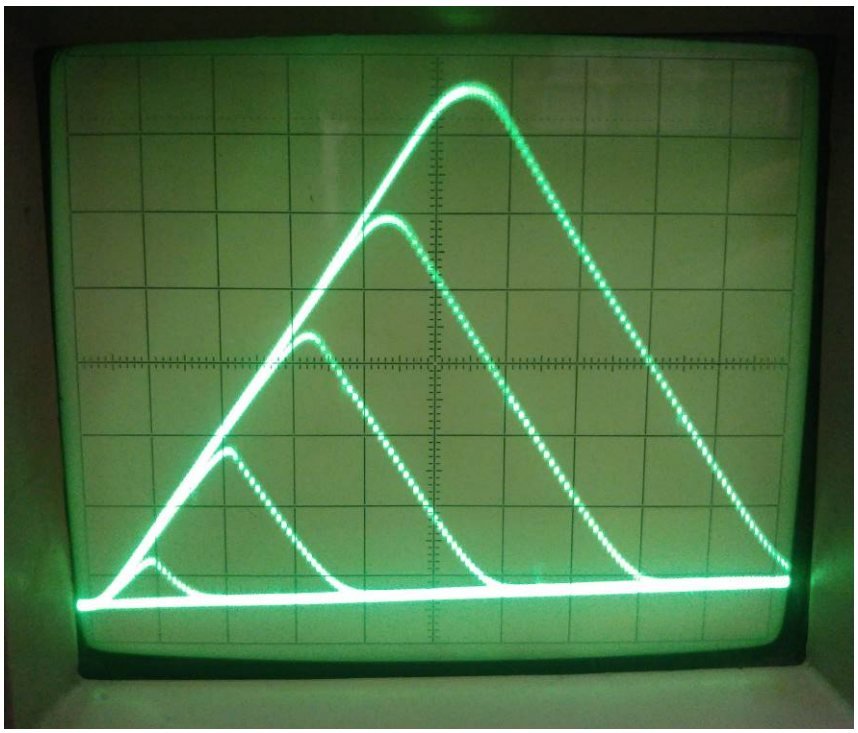

**Figure 29 – Static I-V of the frequency transducer on bipolar transistors (on the vertical one division – 2mA, on the horizontal axis – 2V)**

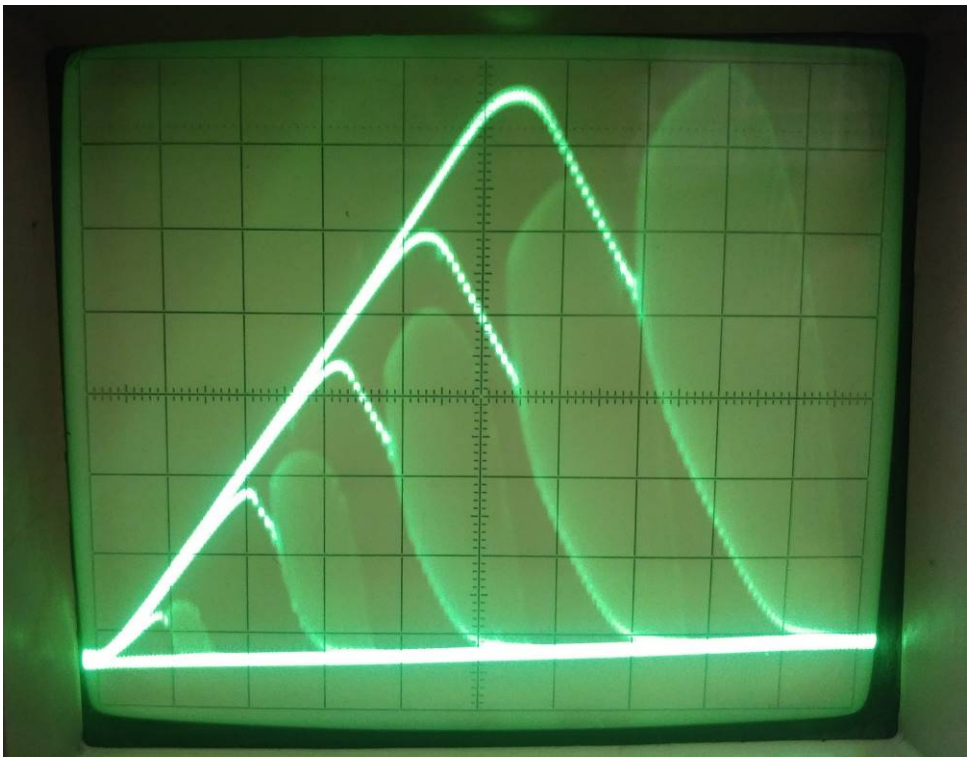

**Figure 30 – Dynamic I-V of the frequency transducer on bipolar transistors (on the vertical axis one division - 2mA, along the horizontal axis – 2V)**

As can be seen from fig. 30, the amplitude of the generated oscillations

approaches the supply voltage. The greater the supply voltage we apply, the greater the amplitude of oscillations we get. Comparing the generated oscillations of fig. 30 with fluctuations in fig. 10, it can be noted that the amplitude of the generated oscillations in the frequency transducer with the field-effect transistor is more stable. This, in turn, will affect the linearity of the transformation function.

For the theoretical conversion function of the magnetic field induction radio measuring transducer at a supply voltage of 5V, we will linearize it. Let's divide the measurement range into two sub-ranges: from 0 to 0.3 T; 0.3 – 1 T. Using the MathCad mathematical package, we obtain the following expressions for the transformation function in the subranges:

$$f_1(B) = 2,4153B + 2665\,;\; f_2(B) = 1,25286B + 3035\,.$$

In fig. 31 shows the theoretical transformation function and approximate lines in the subbands.

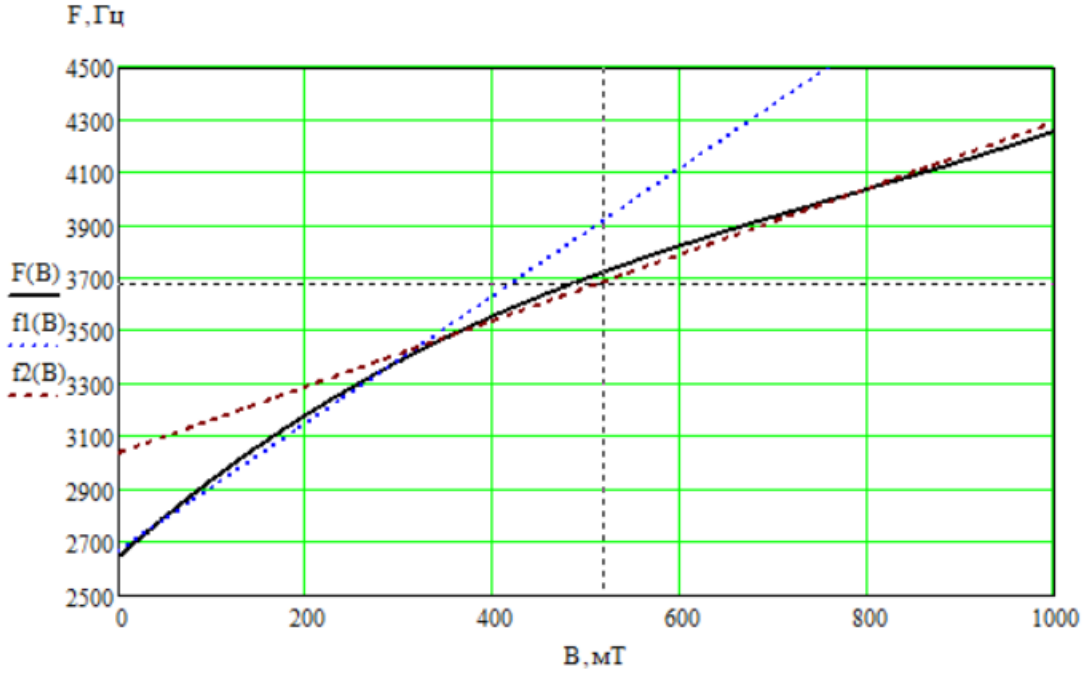


**Figure 31 – Graphs of the theoretical transformation function and its linearization lines in subbands**

Thus, upon linearization of the transformation function, we obtain the following sensitivity values in the subbands:

$$\text{0-0.3 T: } S_1(B) = 2.41\text{kHz/mTl; 0.3-1 T: } S_2(B) = 1.25\text{kHz/mT.}$$

We will calculate the maximum nonlinearity error for each sub-range according to formula (14).

By substituting numerical values, we get for eachsub-range:

$$\gamma_{H1} = \frac{3055 - 3023}{3390 - 2638} = 0,044\,;\; \gamma_{H2} = \frac{3714 - 3677}{4288 - 3412} = 0,043\,.$$

In this case, we obtained almost the same nonlinearity error for both subbands. As we can see from the calculations, for this option, even when divided into only two subbands, we get a slight nonlinearity error compared to the previous radio-measuring frequency transducer. At the same time, we increase the sensitivity of the transducer several times.

## Conclusions

1. The improved mathematical model of the radio-measuring magnetic field transducer, which consists of a Hall sensor and a frequency transducer based on two bipolar and field-effect transistors, made it possible to increase the sensitivity of the magnetic field induction radio-measuring device, which includes such a transducer. In the transducer, the influence of the induction and frequency of the external magnetic field, supply and control voltages on the frequency of the output oscillations of the transducer was taken into account. The sensitivity of the radio measuring device with such a frequency transducer was increased in the range of magnetic field induction measurement 0-200 mT and is 620 Hz/mT.

2. The improved mathematical model of the radio-measuring magnetic field transducer, which consists of a double-collector bipolar magnetotransistor and a frequency transducer based on two bipolar and field-effect transistors, made it possible to reduce the nonlinearity error of both the transducer and the radio-measuring device of magnetic field induction as a whole. In the improved mathematical model of such a transducer of a radio measuring device, the effect of induction and frequency of the external magnetic field, supply and control voltages on the frequency of output oscillations of the transducer was taken into account. This option has the smallest nonlinear error of 1.8% of all three investigated options in the range of magnetic field inductions from 0 to 300 mT.

3. The improved mathematical model of the radio measuring magnetic field transducer, which consists of a two-collector bipolar magnetotransistor and a frequency transducer based on three bipolar transistors, made it possible to increase the sensitivity in the magnetic field induction measurement range of 0-300 mT to a value of 2.41 kHz/mT, in the range of 0 ,3-1 T – up to the value of 1.25 kHz/mT.